

Double-Cover-Based Analysis of the Bethe Permanent of Block-Structured Positive Matrices

Binghong Wu

Department of Information Engineering
The Chinese University of Hong Kong
Shatin, N.T., Hong Kong
wb024@ie.cuhk.edu.hk

Pascal O. Vontobel

Department of Information Engineering
The Chinese University of Hong Kong
Shatin, N.T., Hong Kong
pascal.vontobel@ieee.org

Abstract—We consider the permanent of a square matrix with non-negative entries. A tractable approximation is given by the so-called Bethe permanent that can be efficiently computed by running the sum-product algorithm on a suitable factor graph. While the ratio of the permanent of a matrix to its Bethe permanent is, in the worst case, upper and lower bounded by expressions that are exponentially far apart in the matrix size, in practice it is observed for many ensembles of matrices of interest that this ratio is strongly concentrated around some value that depends only on the matrix size. In this paper, for an ensemble of block-structured matrices where entries in a block take the same value, we numerically study the ratio of the permanent of a matrix to its Bethe permanent. It is observed that also for this ensemble the ratio is strongly concentrated around some value depending only on a few key parameters of the ensemble. We use graph-cover-based approaches to explain the reasons for this behavior and to quantify the observed value.

Index Terms—Permanent, Bethe approximation, normal factor graph, graph covers, analytic combinatorics in several variables (ACSV), pattern maximum likelihood (PML).

I. INTRODUCTION

Let n be a positive integer and let $\mathbf{A} \triangleq (a_{i,j}) \in \mathbb{R}_{\geq 0}^{n \times n}$. The permanent of the matrix \mathbf{A} is defined to be

$$\text{perm}(\mathbf{A}) \triangleq \sum_{\sigma \in \mathcal{S}_n} \prod_{i \in [n]} a_{i, \sigma(i)}, \quad (1)$$

where \mathcal{S}_n is the set of all permutations of $[n] \triangleq \{1, \dots, n\}$. The permanent is a fundamental quantity in combinatorics and statistical physics [1]. In graphical-model terms [2]–[4], one can formulate a graphical model such that its partition function equals $\text{perm}(\mathbf{A})$. Equivalently, $\text{perm}(\mathbf{A})$ is characterized by the minimum of the Gibbs free energy function associated with the graphical model, and therefore we will refer to it as the Gibbs permanent. Computing $\text{perm}(\mathbf{A})$ exactly is #P-hard, motivating efficient surrogates. The Bethe permanent $\text{perm}_B(\mathbf{A})$ is obtained by minimizing the Bethe free energy (or, equivalently, by running the sum-product algorithm (SPA) on a suitable graphical model) [4], [5]. While often remarkably accurate, the Bethe approximation incurs a systematic gap, making the ratio $\text{perm}(\mathbf{A})/\text{perm}_B(\mathbf{A})$ a key quantity to understand.

A main motivation for the investigations in the present paper is the pattern maximum likelihood (PML) problem [6]. Several works [7]–[9] show that determining the PML is

equivalent to computing $\arg \max_{\mathbf{A}} \text{perm}(\mathbf{A})$ over a structured family of non-negative matrices. Since exact permanents are intractable for large matrices, Vontobel [7], [8] proposed the practical surrogate objective $\arg \max_{\mathbf{A}} \text{perm}_B(\mathbf{A})$, which makes it essential to understand the approximation ratio $\text{perm}(\mathbf{A})/\text{perm}_B(\mathbf{A})$ on PML-induced instances. More recently, Anari *et al.* [9] highlighted that these instances possess pronounced low-complexity structure (e.g., few distinct rows/columns, low non-negative rank) and leveraged this viewpoint to justify and analyze scalable surrogates, including both Bethe- and Sinkhorn-type approximations, for approximate PML optimization.

It is therefore of interest to study the ratio $\text{perm}(\mathbf{A})/\text{perm}_B(\mathbf{A})$ for highly structured matrices, in particular for block-structured matrices where all the entries in a block take the same value. A simple instance for such a matrix with $n=5$ and $m=2$ is

$$\mathbf{A} \triangleq \mathbf{A}(\mathbf{B}, \mathbf{k}, \boldsymbol{\ell}) \triangleq \left(\begin{array}{cccc|c} b_{11} & b_{11} & b_{11} & b_{11} & b_{12} \\ b_{11} & b_{11} & b_{11} & b_{11} & b_{12} \\ b_{11} & b_{11} & b_{11} & b_{11} & b_{12} \\ \hline b_{21} & b_{21} & b_{21} & b_{21} & b_{22} \\ b_{21} & b_{21} & b_{21} & b_{21} & b_{22} \end{array} \right), \quad (2)$$

which is based on the matrix $\mathbf{B} \triangleq (b_{i,j}) \in \mathbb{R}_{>0}^{m \times m}$, row block sizes $\mathbf{k} = (k_1, k_2) = (3, 2)$ and column block sizes $\boldsymbol{\ell} = (\ell_1, \ell_2) = (4, 1)$. In the case of the PML, we have $b_{i,j} \triangleq q_i^{\mu_j}$, with probabilities $\{q_i\}_i$ and frequencies $\{\mu_j\}_j$. (See, e.g., [7], [8] for details.)

The Bethe permanent has a substantial literature, ranging from variational viewpoints to approximation guarantees (see, e.g., [9]–[13]). In particular, for an arbitrary matrix $\mathbf{A} \in \mathbb{R}_{\geq 0}^{n \times n}$ it was proven that

$$1 \leq \frac{\text{perm}(\mathbf{A})}{\text{perm}_B(\mathbf{A})} \leq 2^{n/2}, \quad (3)$$

with the lower and upper bounds being tight. In contrast to this substantial gap between the worst case upper and lower bounds, in practice it is observed that for many matrix ensembles of interest the ratio $\text{perm}(\mathbf{A})/\text{perm}_B(\mathbf{A})$ is strongly concentrated. See, e.g., the paper [14], that studied matrices with i.i.d. entries.

In the present paper, we make a similar observation for block-structured matrices $\mathbf{A}(\mathbf{B}, \mathbf{k}, \boldsymbol{\ell})$, see Fig. 1. The results in this figure are obtained as follows: we fix $n=5$ and $m=2$,

and construct $\mathbf{A} \triangleq \mathbf{A}(\mathbf{B}, \mathbf{k}, \boldsymbol{\ell})$ based on \mathbf{B} -matrices whose entries are generated i.i.d. according to some distribution and based on block sizes $\mathbf{k} = (k_1, k_2)$ and $\boldsymbol{\ell} = (\ell_1, \ell_2)$ that are randomly generated. For each such matrix, we draw a blue triangle at the location $(x, y) = (\text{perm}(\mathbf{A}), \text{perm}_{\mathbf{B}}(\mathbf{A}))$. We see that the resulting blue triangles follow closely the line $x \mapsto y \triangleq \sqrt{e/(2\pi n)} \cdot x$, i.e., the ratio $\text{perm}(\mathbf{A})/\text{perm}_{\mathbf{B}}(\mathbf{A})$ is close to $\sqrt{2\pi n}/e$. Interestingly, this ratio is the same as the ratio that was observed for the ensemble under consideration in [14]. These observations reinforce the practical reliability of Bethe-based surrogates on PML-type structured matrices.

While $\text{perm}_{\mathbf{B}}(\mathbf{A})$ can be computed efficiently, it turns out to be rather difficult to characterize this quantity analytically except for a few special cases. This is the reason why in this paper we analyze the degree-2 Bethe permanent $\text{perm}_{\mathbf{B},2}(\mathbf{A})$ of \mathbf{A} instead of $\text{perm}_{\mathbf{B}}(\mathbf{A})$, similar to what was done in [14]. While $\text{perm}_{\mathbf{B},2}(\mathbf{A})$ is different from $\text{perm}_{\mathbf{B}}(\mathbf{A})$, these investigations are valuable because

- the ratio $\text{perm}(\mathbf{A})/\text{perm}_{\mathbf{B},2}(\mathbf{A})$ is predictive of the ratio $\text{perm}(\mathbf{A})/\text{perm}_{\mathbf{B}}(\mathbf{A})$,
- the analysis of $\text{perm}_{\mathbf{B},2}(\mathbf{A})$ gives insights into the value taken by the ratio $\text{perm}(\mathbf{A})/\text{perm}_{\mathbf{B},2}(\mathbf{A})$, and with that insights into the value taken by the ratio $\text{perm}(\mathbf{A})/\text{perm}_{\mathbf{B}}(\mathbf{A})$.

Continuing the above simulation study, Fig. 1 also shows the numerical results for the degree-2 Bethe permanent $\text{perm}_{\mathbf{B},2}(\mathbf{A})$, where a red circle is drawn at the location $(x, y) = (\text{perm}(\mathbf{A}), \text{perm}_{\mathbf{B},2}(\mathbf{A}))$. We see that the resulting red circles follow closely the line $x \mapsto y \triangleq \sqrt[4]{e/(\pi n)} \cdot x$, i.e., the ratio $\text{perm}(\mathbf{A})/\text{perm}_{\mathbf{B},2}(\mathbf{A})$ is close to $\sqrt[4]{\pi n}/e$.

Recall that the degree-2 Bethe permanent $\text{perm}_{\mathbf{B},2}(\mathbf{A})$, and, more generally, the degree- M Bethe permanent $\text{perm}_{\mathbf{B},M}(\mathbf{A})$ are defined as follows [5], [15]. Namely,

$$\text{perm}_{\mathbf{B},M}(\mathbf{A}) \triangleq \sqrt[M]{\left\langle \text{perm}(\mathbf{A}^{\uparrow \tilde{\mathbf{P}}}) \right\rangle_{\tilde{\mathbf{P}} \in \tilde{\Phi}_M}}, \quad (4)$$

where $\langle \cdot \rangle$ is the arithmetic average over all degree- M covers (equivalently, over all cover configurations $\tilde{\mathbf{P}} \in \tilde{\Phi}_M$), and $\mathbf{A}^{\uparrow \tilde{\mathbf{P}}}$ is the corresponding $Mn \times Mn$ lifted matrix. (See [5], [15] for details.) As was shown in [5], [15],

$$\text{perm}_{\mathbf{B},1}(\mathbf{A}) = \text{perm}(\mathbf{A}), \quad (5)$$

$$\limsup_{M \rightarrow \infty} \text{perm}_{\mathbf{B},M}(\mathbf{A}) = \text{perm}_{\mathbf{B}}(\mathbf{A}). \quad (6)$$

It is straightforward to see that one can write

$$\frac{\text{perm}(\mathbf{A})}{\text{perm}_{\mathbf{B}}(\mathbf{A})} = \frac{\text{perm}(\mathbf{A})}{\text{perm}_{\mathbf{B},2}(\mathbf{A})} \cdot \frac{\text{perm}_{\mathbf{B},2}(\mathbf{A})}{\text{perm}_{\mathbf{B}}(\mathbf{A})}. \quad (7)$$

A recurring empirical observation, and a useful working heuristic for asymptotics, is that the two factors on the right-hand side are often very similar [14], [16], [17]. Consequently,

$$\frac{\text{perm}(\mathbf{A})}{\text{perm}_{\mathbf{B}}(\mathbf{A})} \approx \left(\frac{\text{perm}(\mathbf{A})}{\text{perm}_{\mathbf{B},2}(\mathbf{A})} \right)^2, \quad (8)$$

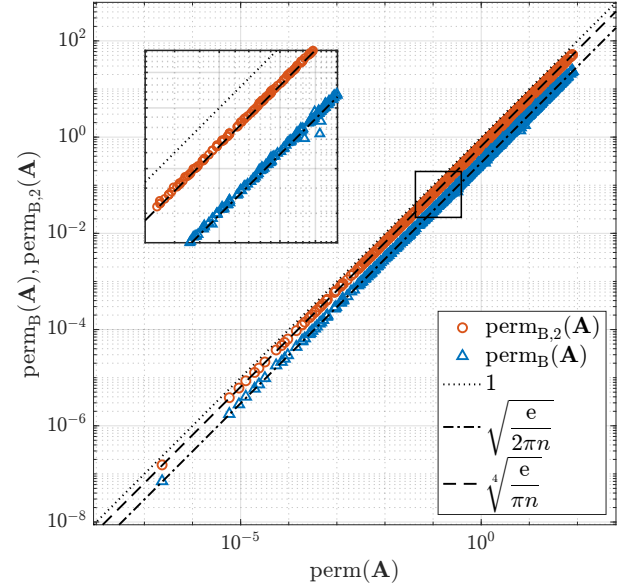


Fig. 1: Numerical results for block-structured matrices \mathbf{A} , along with theoretical asymptotics, for $n=5$ and $m=2$. (See Section I for details.)

and so understanding the ratio $\text{perm}(\mathbf{A})/\text{perm}_{\mathbf{B},2}(\mathbf{A})$ goes a long way toward understanding the ratio $\text{perm}(\mathbf{A})/\text{perm}_{\mathbf{B}}(\mathbf{A})$.

In particular, Ng and Vontobel [14] established the following results. For the all-one matrix $\mathbf{A} \triangleq \mathbf{1}_{n \times n}$, they proved that¹

$$\frac{\text{perm}(\mathbf{A})}{\text{perm}_{\mathbf{B}}(\mathbf{A})} \sim \sqrt{\frac{2\pi n}{e}}, \quad \frac{\text{perm}(\mathbf{A})}{\text{perm}_{\mathbf{B},2}(\mathbf{A})} \sim \sqrt[4]{\frac{\pi n}{e}}, \quad (9)$$

showing analytically that the expression in (8) holds up to a factor $\sqrt{2}$. Moreover, for matrices with i.i.d. entries, they showed that

$$\gamma_{\mathbf{B},2}(n) \triangleq \frac{\sqrt{\mathbb{E}[\text{perm}(\mathbf{A})^2]}}{\sqrt{\mathbb{E}[\text{perm}_{\mathbf{B},2}(\mathbf{A})^2]}} \sim \gamma'_{\mathbf{B},2}(n) \triangleq \sqrt[4]{\frac{\pi n}{e}}. \quad (10)$$

One observes that the ratios $\sqrt{2\pi n}/e$ and $\sqrt[4]{\pi n}/e$ that appear in (9)–(10) also play a key role for the ensemble of matrices that is considered in Fig. 1.

The main result of the present paper is that for a matrix $\mathbf{A} \triangleq \mathbf{A}(\mathbf{B}, \mathbf{k}, \boldsymbol{\ell})$ it holds that

$$\frac{\text{perm}(\mathbf{A})}{\text{perm}_{\mathbf{B},2}(\mathbf{A})} \sim \sqrt[4]{\frac{\pi n}{e}} \cdot \sqrt[4]{\frac{1}{\prod_{i=2}^m e^{\rho_i} (1 - \rho_i)}}, \quad (11)$$

where $\{\rho_i\}_{i=2}^m$ are real numbers in the interval $[0, 1)$ computed based on \mathbf{B} , \mathbf{k} , and $\boldsymbol{\ell}$. For many matrix ensembles $\mathbf{A}(\mathbf{B}, \mathbf{k}, \boldsymbol{\ell})$ of interest (in particular the matrix ensembles of interest in the PML setting), we observe that $\rho_i \ll 1$, $2 \leq i \leq m$, and so

$$\frac{\text{perm}(\mathbf{A})}{\text{perm}_{\mathbf{B},2}(\mathbf{A})} \sim \sqrt[4]{\frac{\pi n}{e}} \cdot \left(1 + O\left(\sum_{i=2}^m \rho_i^2\right) \right). \quad (12)$$

¹The notation $a(n) \sim b(n)$ stands for $\lim_{n \rightarrow \infty} \frac{a(n)}{b(n)} = 1$.

The rest of this paper is structured as follows:

- In Section II, we review the normal factor graph (NFG) representation of the Gibbs and Bethe permanents, and the cycle-index machinery that underpins our analysis.
- In Section III, we formulate the block constraints via multivariate generating functions and apply analytic combinatorics in several variables (ACSV) [18] to obtain the asymptotics.
- In Section IV, we present numerical experiments on representative structured instances from the PML setup, demonstrating the robustness of the predicted ratio.
- In Section V, we conclude the paper and present an outlook.
- All technical proofs and auxiliary derivations are deferred to the appendices.

Notation. We denote the transpose of a matrix \mathbf{M} by \mathbf{M}^T . For $\mathbf{k} \in \mathbb{Z}_{\geq 0}^m$, we define $\mathbf{k}! \triangleq \prod_{i \in [m]} (k_i!)$. For $\mathbf{w} \in \mathbb{R}_{\geq 0}^m$ and $\mathbf{k} \in \mathbb{Z}^m$, we define $\mathbf{w}^{\mathbf{k}} \triangleq \prod_{i \in [m]} w_i^{k_i}$.

II. BACKGROUND:

NFGs, DOUBLE COVERS, AND THE CYCLE INDEX

A. Normal factor graphs and partition sums

A factor graph \mathbf{N} can be used to depict a multivariate function that is the product of (simpler) multivariate functions. The former function is called the global function and the latter functions are called local functions. The corresponding factor graph consists of function nodes and variable nodes, where for each local function one draws a function node, for every variable one draws a variable node, and for every variable appearing as an argument of a local function one draws an edge between the corresponding variable and function nodes. A valid configuration is an assignment of values to the variable nodes such that the global function takes on a nonzero value.

The partition sum $Z(\mathbf{N})$ is defined to be the sum of the global function over all possible variable assignments, or, equivalently, the sum of the global function over all valid configurations. With suitable local functions, partition sums encode many combinatorial quantities of interest.

In the present paper, we use normal factor graphs (NFGs) in the sense of [2], [3], where the factorization is formulated such that all variable nodes have degree two or one, and because of this the variable nodes are then usually omitted in drawings, i.e., there are no variable nodes in drawings, and variables are simply associated with edges or half-edges.

Our analysis builds upon the double-cover NFG framework for the permanent [5], [14]–[17]. We adopt the formulation from these papers, restating here only the key definitions and propositions required for our derivation. (We refer to Appendix A for a much more detailed discussion.) The corresponding graphs are shown in Fig. 2.

B. NFGs for permanents

Given $\mathbf{A} = (a_{i,j}) \in \mathbb{R}_{\geq 0}^{n \times n}$, one builds an NFG $\mathbf{N}(\mathbf{A})$ on the complete bipartite graph, see Fig. 2 (left), with function nodes $\{f_{L,i}\}_{i \in [n]}$ on the left-hand side, function nodes $\{f_{R,j}\}_{j \in [n]}$

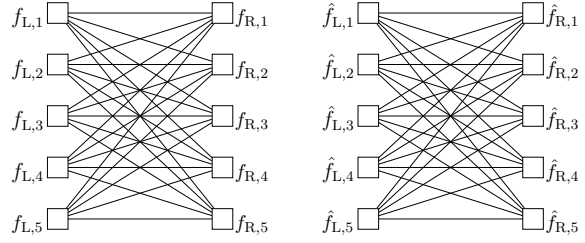


Fig. 2: NFGs used to represent $\text{perm}(\mathbf{A})$ (left) and $\text{perm}_{B,2}(\mathbf{A})$ (right).

on the right-hand side, and, for every $(i, j) \in [n]^2$, the variable $x_{i,j} \in \{0, 1\}$ is associated with the edge connecting $f_{L,i}$ and $f_{R,j}$. The local functions are defined such that they take on a nonzero value if only if exactly one of the variables associated with the incident edges equals 1.² With this, every valid configuration of $\mathbf{N}(\mathbf{A})$ corresponds to a perfect matching in the bipartite graph. In particular, if the perfect matching corresponds to a permutation $\sigma \in \mathcal{S}_n$, then, because of the way that the local functions are defined, the global function equals $\prod_{i \in [n]} a_{i,\sigma(i)}$, and so the partition function of $\mathbf{N}(\mathbf{A})$ satisfies $Z(\mathbf{N}(\mathbf{A})) = \text{perm}(\mathbf{A})$.

The paper [14] defines an NFG $\hat{\mathbf{N}}(\mathbf{A})$, shown in Fig. 2 (right), whose partition sum satisfies $Z(\hat{\mathbf{N}}(\mathbf{A})) = (\text{perm}_{B,2}(\mathbf{A}))^2$. While the graph underlying $\hat{\mathbf{N}}(\mathbf{A})$ is the same as the graph underlying $\mathbf{N}(\mathbf{A})$ in Fig. 2 (left), its variable alphabets and local functions are different. Namely, for every $(i, j) \in [n]^2$,

$$\hat{x}_{i,j} \in \{0, 1\}^2 = \{(0, 0), (0, 1), (1, 0), (1, 1)\}, \quad (13)$$

and with the definition of the local functions appearing in Appendix A. The properties of these local functions turn out to have the following important implication for the valid configurations of $\hat{\mathbf{N}}(\mathbf{A})$. Namely, after disregarding edges whose associated variable take the value $(0, 0)$, every valid configuration of $\hat{\mathbf{N}}(\mathbf{A})$ consists of disconnected components corresponding to

- single edges whose associated variable takes the value $(1, 1)$,
- simple cycles whose associated variables take the value $(0, 1)$,

and with every function node being part of one of these disconnected components. Crucially, the value $(1, 0)$ does not appear in any valid configuration.

Similar to the construction of $\hat{\mathbf{N}}(\mathbf{A})$, an NFG can be constructed such that its partition sum equals $(\text{perm}(\mathbf{A}))^2$. This NFG has local function nodes that have the following important implication for the valid configurations. Namely, after disregarding edges whose associated variable take the value $(0, 0)$, every valid configuration of $\hat{\mathbf{N}}(\mathbf{A})$ consists of disconnected components corresponding to

²In order to avoid awkward language, we assume that $a_{i,j} > 0$, $(i, j) \in [n]^2$ in this description.

- single edges whose associated variable takes the value $(1, 1)$,
- simple cycles whose associated variables take the value $(0, 1)$,
- simple cycles whose associated variables take the value $(1, 0)$,

and with every function node being part of one of these disconnected components.

With the help of $\hat{N}(\mathbf{A})$, Ng and Vontobel [14, Proposition 2] show that

$$\frac{(\text{perm}(\mathbf{A}))^2}{(\text{perm}_{B,2}(\mathbf{A}))^2} = \left(\sum_{\sigma_1, \sigma_2 \in \mathcal{S}_n} p(\sigma_1) p(\sigma_2) 2^{-c(\sigma_1 \circ \sigma_2^{-1})} \right)^{-1}, \quad (14)$$

where $p(\sigma) \triangleq (\prod_{i \in [n]} a_{i, \sigma(i)}) / \text{perm}(\mathbf{A})$ and where $c(\sigma)$ is the number of cycles of length at least two in σ .³ Note that the term $2^{-c(\sigma_1 \circ \sigma_2^{-1})}$ is the result of the non-existence of $(1, 0)$ -cycles in the valid configurations of $\hat{N}(\mathbf{A})$. In particular,

- without the term $2^{-c(\sigma_1 \circ \sigma_2^{-1})}$, the expression on the right-hand side of Eq. (14) is equal to 1,
- with the term $2^{-c(\sigma_1 \circ \sigma_2^{-1})}$, the expression on the right-hand side of Eq. (14) is at least 1.

With this, Eq. (14) shows the clear influence of the cycles in $\hat{N}(\mathbf{A})$ on the ratio $\text{perm}(\mathbf{A}) / \text{perm}_{B,2}(\mathbf{A})$.

Eq. (14) will serve as our main black-box tool. Since the weight depends on (σ_1, σ_2) only through the cycle structure of $\sigma_1 \circ \sigma_2^{-1}$, it naturally leads to a cycle-index organization, where the factor $1/2$ per non-trivial cycle becomes a simple substitution at the level of generating functions.

III. POSITIVE BLOCK-CONSTANT MODEL

We now specialize to positive block-constant matrices with fixed row and column partitions and set up the multivariate coefficient-extraction framework used in the subsequent analysis.

Assumption 1. Let n and m be positive integers. Fix positive integer vectors $\mathbf{k}, \mathbf{\ell} \in \mathbb{Z}_{>0}^m$ such that $\sum_{i \in [m]} k_i = \sum_{j \in [m]} \ell_j = n$ and fix the matrix $\mathbf{B} \triangleq (b_{i,j}) \in \mathbb{R}_{>0}^{m \times m}$. The block-constant matrix $\mathbf{A} \triangleq \mathbf{A}(\mathbf{B}, \mathbf{k}, \mathbf{\ell}) \in \mathbb{R}_{>0}^{n \times n}$ is defined to be the matrix that is obtained by expanding each $b_{i,j}$ into a constant-value block of size $k_i \times \ell_j$, i.e.,

$$\mathbf{A} \triangleq \begin{pmatrix} b_{1,1} \mathbf{1}_{k_1 \times \ell_1} & \cdots & b_{1,m} \mathbf{1}_{k_1 \times \ell_m} \\ \vdots & \ddots & \vdots \\ b_{m,1} \mathbf{1}_{k_m \times \ell_1} & \cdots & b_{m,m} \mathbf{1}_{k_m \times \ell_m} \end{pmatrix}, \quad (15)$$

where $\mathbf{1}_{k \times \ell}$ denotes the all-one matrix of size $k \times \ell$.

To capture the combinatorics of closed walks on $\hat{N}(\mathbf{A})$, we introduce indeterminates $\mathbf{t} = (t_1, \dots, t_m)$ and $\mathbf{u} = (u_1, \dots, u_m)$ as counting indeterminates in the generating

³If $\sigma \in \mathcal{S}_6$ is such that $\sigma(1) = 2, \sigma(2) = 3, \sigma(3) = 1, \sigma(4) = 5, \sigma(5) = 4, \sigma(6) = 6$, then in cycle notation σ reads $(123)(45)(6)$, showing that σ consists of one cycle of length 3, one cycle of length 2, and one cycle of length 1, and with this $c(\sigma) = 2$.

functions, marking row and column types so that the partitioning $(\mathbf{k}, \mathbf{\ell})$ is selected by $[\mathbf{t}^\mathbf{k} \mathbf{u}^\mathbf{\ell}]$.

Definition 2. The fundamental matrix governing the walk transitions is the $m \times m$ weighted transition matrix \mathbf{W} , defined by

$$\mathbf{W} \triangleq \mathbf{B}^\top \cdot \text{diag}(\mathbf{t}) \cdot \mathbf{B} \cdot \text{diag}(\mathbf{u}). \quad (16)$$

The total weight of length- h closed walks can be expressed by $\text{tr}(\mathbf{W}^h)$.

Our analysis will rely on the spectrum of \mathbf{W} and the values of $\text{tr}(\mathbf{W}^h)$, $h \in \mathbb{Z}_{\geq 0}$. Now, while the matrix \mathbf{W} encodes the relevant walk weights, in order to have a better handle on the spectrum, we prefer working with a symmetric matrix. Fortunately, such a matrix \mathbf{S} can be obtained by applying a similarity transform to \mathbf{W} . Note that, thanks to the cyclic invariance of the trace, $\text{tr}(\mathbf{W}^h) = \text{tr}(\mathbf{S}^h)$, $h \in \mathbb{Z}_{\geq 0}$.

Definition 3. We define the symmetric state-transition matrix $\mathbf{S} \triangleq \mathbf{S}(\mathbf{t}, \mathbf{u})$ of size $m \times m$ by

$$\begin{aligned} \mathbf{S} &\triangleq \text{diag}(\mathbf{u})^{1/2} \cdot \mathbf{W} \cdot \text{diag}(\mathbf{u})^{-1/2} \\ &= \text{diag}(\mathbf{u})^{1/2} \cdot \mathbf{B}^\top \cdot \text{diag}(\mathbf{t}) \cdot \mathbf{B} \cdot \text{diag}(\mathbf{u})^{1/2}. \end{aligned} \quad (17)$$

Let $\lambda_1, \dots, \lambda_m$ be the eigenvalues of \mathbf{W} and \mathbf{S} . (Because \mathbf{S} and \mathbf{W} are similar matrices, they share the spectrum.) With this, $\text{tr}(\mathbf{S}^h) = \text{tr}(\mathbf{W}^h) = \sum_{i \in [m]} \lambda_i^h$ for $h \geq 0$. Moreover, when $\mathbf{t}, \mathbf{u} \in \mathbb{R}_{>0}^m$ (as will hold at the dominant point identified later), the matrix $\mathbf{S}(\mathbf{t}, \mathbf{u})$ is real symmetric and positive semi-definite, and so, without loss of generality, we can assume that $\lambda_1 \geq \lambda_2 \geq \dots \geq \lambda_m \geq 0$. Under the strict-positivity assumption on \mathbf{B} (and \mathbf{t}, \mathbf{u}), Perron–Frobenius theory yields a leading eigenvalue λ_1 with a spectral gap, i.e., $\lambda_1 > \lambda_2$. For details from a factor-graph perspective, please see Appendix B.

Cycle-index-based generating functions can be used to analyze $(\text{perm}(\mathbf{A}))^2$ and $(\text{perm}_{B,2}(\mathbf{A}))^2$ based on the observations before Eq. (14) and Eq. (14) itself, as shown in the following two lemmas.

Lemma 4. Under Assumption 1 and Definition 3, let (\mathbf{t}, \mathbf{u}) be such that $\mathbf{t}, \mathbf{u} \in \mathbb{R}_{>0}^m$ and $\lambda_1(\mathbf{S}(\mathbf{t}, \mathbf{u})) < 1$. Define

$$C^G(\mathbf{t}, \mathbf{u}) \triangleq \exp \left(\sum_{h \geq 1} \frac{\text{tr}(\mathbf{S}(\mathbf{t}, \mathbf{u})^h)}{h} \right), \quad (18)$$

$$C^B(\mathbf{t}, \mathbf{u}) \triangleq \exp \left(\text{tr}(\mathbf{S}(\mathbf{t}, \mathbf{u})) + \sum_{h \geq 2} \frac{\text{tr}(\mathbf{S}(\mathbf{t}, \mathbf{u})^h)}{2h} \right). \quad (19)$$

Then

$$C^G(\mathbf{t}, \mathbf{u}) = \frac{1}{\det(\mathbf{I} - \mathbf{S}(\mathbf{t}, \mathbf{u}))}, \quad (20)$$

$$C^B(\mathbf{t}, \mathbf{u}) = \frac{\exp(\frac{1}{2} \text{tr}(\mathbf{S}(\mathbf{t}, \mathbf{u})))}{\sqrt{\det(\mathbf{I} - \mathbf{S}(\mathbf{t}, \mathbf{u}))}}. \quad (21)$$

Proof. The result uses that for $\mathbf{t}, \mathbf{u} \in \mathbb{R}_{>0}^m$ such that $\lambda_1(\mathbf{S}(\mathbf{t}, \mathbf{u})) < 1$, the expansion $\log(\mathbf{I} - \mathbf{S}) = -\sum_{h \geq 1} \mathbf{S}^h/h$

converges. Moreover, for any square matrix \mathbf{M} , it holds that $\exp(\text{tr}(\mathbf{M})) = \det(\exp(\mathbf{M}))$. \square

Lemma 5. Consider the matrix $\mathbf{A} \triangleq \mathbf{A}(\mathbf{B}, \mathbf{k}, \ell)$ from Assumption 1. It holds that

$$(\text{perm}(\mathbf{A}))^2 = \mathbf{k}! \cdot \ell! \cdot Z_n^G(\mathbf{k}, \ell), \quad (22)$$

$$(\text{perm}_{B,2}(\mathbf{A}))^2 = \mathbf{k}! \cdot \ell! \cdot Z_n^B(\mathbf{k}, \ell), \quad (23)$$

where

$$Z_n^G(\mathbf{k}, \ell) = [\mathbf{t}^\mathbf{k} \mathbf{u}^\ell] C^G(\mathbf{t}, \mathbf{u}), \quad (24)$$

$$Z_n^B(\mathbf{k}, \ell) = [\mathbf{t}^\mathbf{k} \mathbf{u}^\ell] C^B(\mathbf{t}, \mathbf{u}). \quad (25)$$

Here, $[\mathbf{t}^\mathbf{k} \mathbf{u}^\ell] C^G(\mathbf{t}, \mathbf{u})$ is the coefficient $c_{\mathbf{k}, \ell}$ of the monomial $\mathbf{c}_{\mathbf{k}, \ell} \mathbf{t}^\mathbf{k} \mathbf{u}^\ell$ in the power series expansion of $C^G(\mathbf{t}, \mathbf{u})$, with a similar interpretation for $[\mathbf{t}^\mathbf{k} \mathbf{u}^\ell] C^B(\mathbf{t}, \mathbf{u})$.

Proof. The coefficients $Z_n^G(\mathbf{k}, \ell)$ and $Z_n^B(\mathbf{k}, \ell)$ arise from the cycle-index enumeration driven by $\mathbf{S}(\mathbf{t}, \mathbf{u})$, hence depend only on the $m \times m$ matrix \mathbf{B} . However, they do not account for the $k_i \times \ell_j$ block repetitions in $\mathbf{A}(\mathbf{B}, \mathbf{k}, \ell)$. Restoring labels within each row/column type class contributes the multiplicity factor $\mathbf{k}! \cdot \ell!$ for both $(\text{perm}(\mathbf{A}))^2$ and $(\text{perm}_{B,2}(\mathbf{A}))^2$, thereby yielding (22)–(23). \square

Proposition 6. Let $\mathbf{z} \triangleq (\mathbf{t}, \mathbf{u})$ denote the set of $2m$ counting indeterminates. Let $\mathbf{w} \triangleq (\mathbf{t}^*, \mathbf{u}^*) \in \mathbb{R}_{>0}^{2m}$ be the unique positive solution to the saddle point equations associated with the partitioning $\mathbf{r} \triangleq (\mathbf{k}, \ell)$. Let $\lambda_1 > \lambda_2 \geq \dots \geq \lambda_m \geq 0$ be the eigenvalues of the matrix $\mathbf{S}(\mathbf{w}) = \mathbf{S}(\mathbf{t}^*, \mathbf{u}^*)$. Defining the spectral ratios $\rho_i \triangleq \lambda_i/\lambda_1$ at the saddle point, the coefficient extraction yields

$$Z_n^G \sim \frac{\mathbf{w}^{-\mathbf{r}}}{\sqrt{(2\pi\|\mathbf{r}\|_2)^{2m-2} \det(\mathcal{H})}} \cdot \frac{\prod_{i=2}^m (1 - \rho_i)^{-1}}{\|\nabla_{\log} Q(\mathbf{w})\|_2}, \quad (26)$$

$$Z_n^B \sim \frac{\mathbf{w}^{-\mathbf{r}}}{\sqrt{(2\pi\|\mathbf{r}\|_2)^{2m-2} \det(\mathcal{H})}} \cdot \frac{\sqrt{\prod_{i=2}^m e^{\rho_i} (1 - \rho_i)^{-1}}}{\|\nabla_{\log} Q(\mathbf{w})\|_2} \cdot \sqrt{\frac{e}{\pi n}}, \quad (27)$$

as $n \rightarrow \infty$, where $\det(\mathcal{H})$ denotes the determinant of the $(2m-2) \times (2m-2)$ Hessian matrix restricted to the tangent space of the singular manifold at \mathbf{w} , and $Q(\mathbf{z}) \triangleq 1 - \lambda_1(\mathbf{z})$ defines this dominant singular manifold.⁴

Proof. See Appendix C. \square

Combining the above results, yields the following theorem.

Theorem 7. Consider the matrix $\mathbf{A} \triangleq \mathbf{A}(\mathbf{B}, \mathbf{k}, \ell)$ from Assumption 1. Let $\rho_i \triangleq \lambda_i/\lambda_1$, $i = 2, \dots, m$, be defined as in Proposition 6. As $n \rightarrow \infty$, it holds that

$$\frac{\text{perm}(\mathbf{A})}{\text{perm}_{B,2}(\mathbf{A})} \sim \sqrt[4]{\frac{\pi n}{e}} \cdot \sqrt[4]{\frac{1}{\prod_{i=2}^m e^{\rho_i} (1 - \rho_i)}}. \quad (28)$$

Proof. The statement follows by combining Proposition 6 with (22)–(23) and taking the square root. \square

⁴Regarding the exponent of $\|\nabla_{\log} Q(\mathbf{w})\|_2$, refer to Remark 9 in Appendix C for a scaling verification.

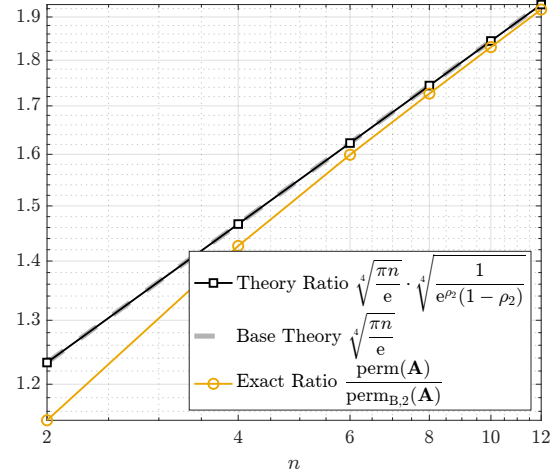


Fig. 3: Numerical results discussed in Section IV.

Corollary 8. We consider the same setup as in Theorem 7. If $\rho_2 \ll 1$, then

$$\frac{\text{perm}(\mathbf{A})}{\text{perm}_{B,2}(\mathbf{A})} \sim \sqrt[4]{\frac{\pi n}{e}} \cdot \left(1 + O\left(\sum_{i=2}^m \rho_i^2\right) \right). \quad (29)$$

Proof. Obtained by applying a Taylor expansion to (28) in the regime $\rho_2 \ll 1$. \square

IV. NUMERICAL VALIDATION

To validate our theory, we consider the following setup:

- The integer n takes the values 2, 4, 6, 8, 10, 12.
- The integer m takes the value 2.
- The partitionings take the values $\mathbf{k} = \ell = (n/2, n/2)$.
- The matrix \mathbf{B} has entries $b_{i,j} = q_i^{\mu_j}$ with $(q_1, q_2) = (0.6, 0.4)$ and $(\mu_1, \mu_2) = (2, 1)$.

For each n , we numerically determine the positive saddle point $(\mathbf{t}^*, \mathbf{u}^*)$ associated with the partitioning (\mathbf{k}, ℓ) , and evaluate the spectrum of the symmetric state-transition matrix $\mathbf{S}(\mathbf{t}^*, \mathbf{u}^*)$. For the above setup, we observe that the spectral ratio is small (numerically, $\rho_2 \approx 0.0102$), making the ρ_i -based correction factor in Theorem 7 negligible. As shown in Fig. 3, the ratio $\text{perm}(\mathbf{A})/\text{perm}_{B,2}(\mathbf{A})$ closely follows the predicted $\sqrt[4]{\pi n/e}$ asymptotic scaling already for the small values of n .

V. CONCLUSION AND OUTLOOK

The results in this paper significant extend the classes of matrices for which the ratio $\text{perm}(\mathbf{A})/\text{perm}_{B,2}(\mathbf{A})$ can be analyzed, and thereby giving insights on the ratio $\text{perm}(\mathbf{A})/\text{perm}_{\mathbf{B}}(\mathbf{A})$.

Thanks to the fact that the saddle point $(\mathbf{t}^*, \mathbf{u}^*)$ is obtained with the help of the Sinkhorn scaling algorithm (see Appendix D), and the fact that the SPA behaves very similar to the Sinkhorn scaling algorithm for the matrices under consideration in this paper, one avenue for future investigations will be about making this connection precise enough such that results about $\text{perm}(\mathbf{A})/\text{perm}_{\mathbf{B}}(\mathbf{A})$ can be derived that are as accurate as the results that are available for $\text{perm}(\mathbf{A})/\text{perm}_{B,2}(\mathbf{A})$.

REFERENCES

- [1] H. Minc, *Permanents*. Reading, MA: Addison-Wesley, 1978.
- [2] F. R. Kschischang, B. J. Frey, and H.-A. Loeliger, “Factor graphs and the sum-product algorithm,” *IEEE Trans. Inf. Theory*, vol. 47, no. 2, pp. 498–519, Feb. 2001.
- [3] H.-A. Loeliger, “An introduction to factor graphs,” *IEEE Sig. Proc. Mag.*, vol. 21, no. 1, pp. 28–41, Jan. 2004.
- [4] J. S. Yedidia, W. T. Freeman, and Y. Weiss, “Constructing free-energy approximations and generalized belief propagation algorithms,” *IEEE Trans. Inf. Theory*, vol. 51, no. 7, pp. 2282–2312, Jul. 2005.
- [5] P. O. Vontobel, “The Bethe permanent of a nonnegative matrix,” *IEEE Trans. Inf. Theory*, vol. 59, no. 3, pp. 1866–1901, 2013.
- [6] A. Orlitsky, N. P. Santhanam, K. Viswanathan, and J. Zhang, “On modeling profiles instead of values,” in *Proceedings of the 20th Conference on Uncertainty in Artificial Intelligence*, ser. UAI ’04. Arlington, Virginia, USA: AUAI Press, 2004, p. 426–435.
- [7] P. O. Vontobel, “The Bethe approximation of the pattern maximum likelihood distribution,” in *Proc. IEEE Int. Symp. Inf. Theory*, Cambridge, MA, USA, 1–6 Jul 2012, pp. 2012–2016.
- [8] ———, “The Bethe and Sinkhorn approximations of the pattern maximum likelihood estimate and their connections to the Valiant–Valiant estimate,” in *Proc. Inf. Theory and Appl. Workshop*, UC San Diego, La Jolla, CA, USA, 9–14 Feb 2014, pp. 1–10.
- [9] N. Anari, M. Charikar, K. Shiragur, and A. Sidford, “The Bethe and Sinkhorn permanents of low rank matrices and implications for profile maximum likelihood,” in *Proc. 34th Conf. Learn. Theory*, ser. Proc. Mach. Learn. Res., M. Belkin and S. Kpotufe, Eds., vol. 134, Boulder, CO, USA, Aug. 15–19 2021, pp. 93–158.
- [10] L. Gurvits, “Unleashing the power of Schrijver’s permanental inequality with the help of the Bethe approximation,” *Elec. Coll. Comp. Compl.*, Dec. 2011.
- [11] L. Gurvits and A. Samorodnitsky, “Bounds on the permanent and some applications,” in *Proc. IEEE Symp. Found. Comp. Sci.*, Philadelphia, PA, USA, Oct. 18–21 2014.
- [12] N. Anari and A. Rezaei, “A tight analysis of Bethe approximation for permanent,” in *Proc. IEEE Ann. Symp. on Found. Comp. Sci.*, 2019, pp. 1434–1445.
- [13] D. Straszak and N. K. Vishnoi, “Belief propagation, Bethe approximation, and polynomials,” *IEEE Trans. Inf. Theory*, vol. 65, no. 7, pp. 4353–4363, Jul. 2019.
- [14] K. S. Ng and P. O. Vontobel, “Double-cover-based analysis of the Bethe permanent of non-negative matrices,” in *Proc. IEEE Inf. Theory Workshop*, Mumbai, India, Nov. 1–9 2022, pp. 1–6.
- [15] P. O. Vontobel, “Counting in graph covers: A combinatorial characterization of the Bethe entropy function,” *IEEE Trans. Inf. Theory*, vol. 59, no. 9, pp. 6018–6048, 2013.
- [16] ———, “Analysis of double covers of factor graphs,” in *Proc. Int. Conf. Sig. Proc. and Comm.*, Bangalore, India, 12–15 Jun 2016, pp. 1–5.
- [17] ———, “Understanding the ratio of the partition sum to its Bethe approximation via double covers,” in *Proc. IEEE Inf. Theory Workshop*, Sydney, Australia, Sep./Oct. 2025, pp. 68–73.
- [18] R. Pemantle, M. C. Wilson, and S. Melczer, *Analytic Combinatorics in Several Variables*, 2nd ed. Cambridge University Press, 2024.
- [19] P. Flajolet and R. Sedgewick, *Analytic Combinatorics*, 1st ed. USA: Cambridge University Press, 2009.
- [20] R. Pemantle and M. C. Wilson, *Analytic Combinatorics in Several Variables*, 1st ed. Cambridge University Press, 2013.
- [21] R. Sinkhorn, “A relationship between arbitrary positive matrices and doubly stochastic matrices,” *The annals of mathematical statistics*, vol. 35, no. 2, pp. 876–879, 1964.
- [22] T. Kato, *Perturbation Theory for Linear Operators*. Springer Science & Business Media, 2013, vol. 132.
- [23] Y. Huang, N. Kashyap, and P. O. Vontobel, “Degree- M Bethe and Sinkhorn permanent based bounds on the permanent of a non-negative matrix,” *IEEE Transactions on Information Theory*, vol. 70, no. 7, pp. 5289–5308, 2024.
- [24] G. P. Egorychev, “The solution of van der Waerden’s problem for permanents,” *Adv. Math.*, vol. 42, pp. 299–305, 1981.
- [25] D. I. Falikman, “Proof of the van der Waerden conjecture regarding the permanent of a doubly stochastic matrix,” *Mathematical Notes of the Academy of Sciences of the USSR*, vol. 29, no. 6, pp. 475–479, Jun. 1981.

APPENDIX A

DETAILED NFG AND DOUBLE-COVER DEFINITIONS

This section collects the normal factor graph (NFG) definitions and the double-cover construction that underlie the cycle-index viewpoint used in the main text. We follow [4], [5], [14]–[17] and mainly focus on [14].

A. NFG $\mathbf{N}(\mathbf{A})$ whose partition function equals $\text{perm}(\mathbf{A})$

Let $\mathbf{A} = (a_{i,j})$ be an arbitrary non-negative matrix of size $n \times n$. We use the NFG $\mathbf{N}(\mathbf{A})$ shown in Fig. 2 (left), which is the same as in [14]:

- $\mathbf{N}(\mathbf{A})$ is based on the complete bipartite graph with n left nodes $\{f_{L,i}\}_{i \in [n]}$ and n right nodes $\{f_{R,j}\}_{j \in [n]}$.
- For $i, j \in [n]$, the edge $(f_{L,i}, f_{R,j})$ carries a binary variable $x_{i,j} \in \mathcal{X} \triangleq \{0, 1\}$.
- For $i \in [n]$, let

$$f_{L,i}(x_{i,1}, \dots, x_{i,n}) \triangleq \begin{cases} \sqrt{a_{i,j}} & \exists j \in [n] \text{ s.t. } x_{i,j} = 1; \\ 0 & x_{i,j'} = 0, \forall j' \in [n] \setminus \{j\} \\ 0 & \text{otherwise} \end{cases}$$

For $j \in [n]$, let

$$f_{R,j}(x_{1,j}, \dots, x_{n,j}) \triangleq \begin{cases} \sqrt{a_{i,j}} & \exists i \in [n] \text{ s.t. } x_{i,j} = 1; \\ 0 & x_{i',j} = 0, \forall i' \in [n] \setminus \{i\} \\ 0 & \text{otherwise} \end{cases}$$

- The global function and the partition function are

$$g(x_{1,1}, \dots, x_{n,n}) \triangleq \left(\prod_{i \in [n]} f_{L,i} \right) \cdot \left(\prod_{j \in [n]} f_{R,j} \right),$$

$$Z(\mathbf{N}) \triangleq \sum_{x_{1,1}, \dots, x_{n,n}} g(x_{1,1}, \dots, x_{n,n}).$$

One checks that $g(x) = \prod_{i \in [n]} a_{i,\sigma(i)}$ if and only if the 1-entries $\{x_{i,\sigma(i)}\}_{i \in [n]}$ form a permutation pattern, and $g(x) = 0$ otherwise. Therefore

$$Z(\mathbf{N}(\mathbf{A})) = \text{perm}(\mathbf{A}). \quad (30)$$

B. Graph Cover Characterization of the Bethe Approximation

For NFGs with non-negative local functions, the Bethe approximation $Z_B(\mathbf{N})$ admits the graph-cover characterization [14]

$$Z_B(\mathbf{N}) = \limsup_{M \rightarrow \infty} Z_{B,M}(\mathbf{N}),$$

$$Z_{B,M}(\mathbf{N}) \triangleq \sqrt[M]{\langle Z(\tilde{\mathbf{N}}) \rangle_{\tilde{\mathbf{N}} \in \tilde{\mathcal{N}}_M}},$$

where the average is over all M -covers $\tilde{\mathbf{N}}$ of \mathbf{N} , $M \geq 1$. Specializing to matrices yields the (degree- M) Bethe permanent

$$\text{perm}_{B,M}(\mathbf{A}) \triangleq \sqrt[M]{\langle \text{perm}(\mathbf{A}^{\uparrow \tilde{\mathbf{P}}}) \rangle_{\tilde{\mathbf{P}} \in \tilde{\Phi}_M}},$$

with

$$\mathbf{A}^{\uparrow \tilde{\mathbf{P}}} \triangleq \begin{pmatrix} a_{1,1} \tilde{\mathbf{P}}^{(1,1)} & \dots & a_{1,n} \tilde{\mathbf{P}}^{(1,n)} \\ \vdots & & \vdots \\ a_{n,1} \tilde{\mathbf{P}}^{(n,1)} & \dots & a_{n,n} \tilde{\mathbf{P}}^{(n,n)} \end{pmatrix},$$

$$\tilde{\Phi}_M \triangleq \left\{ \tilde{\mathbf{P}} = \{\tilde{\mathbf{P}}^{(i,j)}\}_{i \in [n], j \in [n]} \mid \tilde{\mathbf{P}}^{(i,j)} \in \mathcal{P}_{M \times M} \right\},$$

where $\mathcal{P}_{M \times M}$ denotes the set of $M \times M$ permutation matrices. Note that $\mathbf{A}^{\uparrow \tilde{\mathbf{P}}}$ has size $(Mn) \times (Mn)$.

C. The explicit double cover $\hat{\mathbf{N}}(\mathbf{A})$ and its partition function

For the specific case of $M = 2$, there exists an explicit NFG $\hat{\mathbf{N}}(\mathbf{A})$ defined on the same bipartite graph structure as $\mathbf{N}(\mathbf{A})$ shown in Fig. 2 (right). The construction of this graph relies on a specific change of basis detailed in [14].

Conceptually, the degree-2 Bethe permanent involves averaging over graph covers where edge variables represent 4×4 permutation matrices, allowing for parallel (no-cross) or crossed connections. The construction in [14] applies an invertible transformation to the local functions, mapping the state space of these coupled variables into a new basis. A key property of this transformation is that, due to the constraints enforcing perfect matchings, the local functions evaluate to zero for the value $(1, 0)$. Consequently, cycles whose associated variables take the value $(1, 0)$ effectively carry zero weight and do not appear in any valid configuration.

Formally, this results in an NFG $\hat{\mathbf{N}}(\mathbf{A})$ whose partition function satisfies [14, Proposition 1]

$$\text{perm}_{B,2}(\mathbf{A}) = \sqrt{Z(\hat{\mathbf{N}}(\mathbf{A}))}. \quad (31)$$

The edge variables are defined as pairs

$$\hat{x}_{i,j} \in \hat{\mathcal{X}} \triangleq \mathcal{X} \times \mathcal{X} = \{(0,0), (0,1), (1,0), (1,1)\},$$

where $\mathcal{X} \triangleq \{0, 1\}$. Based on the cancellation of the $(1, 0)$ terms described above, the local functions $\hat{f}_{L,i}$ and $\hat{f}_{R,j}$ are given explicitly as follows:

- For $i \in [n]$, define $\hat{f}_{L,i}(\hat{x}_{i,1}, \dots, \hat{x}_{i,n})$ by

$$\hat{f}_{L,i} \triangleq \begin{cases} a_{i,j} & \exists j \in [n] \text{ s.t. } \hat{x}_{i,j} = (1,1); \\ & \hat{x}_{i,j'} = (0,0), \forall j' \in [n] \setminus \{j\} \\ \sqrt{a_{i,j} a_{i,j'}} & \exists j, j' \in [n], j \neq j', \text{ s.t.} \\ & \hat{x}_{i,j} = (0,1), \hat{x}_{i,j'} = (0,1); \\ & \hat{x}_{i,j''} = (0,0), \forall j'' \in [n] \setminus \{j, j'\} \\ 0 & \text{otherwise} \end{cases}$$

- For $j \in [n]$, define $\hat{f}_{R,j}(\hat{x}_{1,j}, \dots, \hat{x}_{n,j})$ by

$$\hat{f}_{R,j} \triangleq \begin{cases} a_{i,j} & \exists i \in [n] \text{ s.t. } \hat{x}_{i,j} = (1,1); \\ & \hat{x}_{i',j} = (0,0), \forall i' \in [n] \setminus \{i\} \\ \sqrt{a_{i,j} a_{i',j}} & \exists i, i' \in [n], i \neq i', \text{ s.t.} \\ & \hat{x}_{i,j} = (0,1), \hat{x}_{i',j} = (0,1); \\ & \hat{x}_{i'',j} = (0,0), \forall i'' \in [n] \setminus \{i, i'\} \\ 0 & \text{otherwise} \end{cases}$$

- The global function and partition function are

$$\hat{g}(\hat{x}_{1,1}, \dots, \hat{x}_{n,n}) \triangleq \left(\prod_{i \in [n]} \hat{f}_{L,i} \right) \cdot \left(\prod_{j \in [n]} \hat{f}_{R,j} \right),$$

$$Z(\hat{N}) \triangleq \sum_{\hat{x}_{1,1}, \dots, \hat{x}_{n,n}} \hat{g}(\hat{x}_{1,1}, \dots, \hat{x}_{n,n}).$$

D. Combinatorial Interpretation via the Cycle Penalty

To understand the difference between $(\text{perm}(\mathbf{A}))^2$ and $(\text{perm}_{B,2}(\mathbf{A}))^2$, we compare the partition sum of the restricted NFG defined above with that of the squared permanent $(\text{perm}(\mathbf{A}))^2$.

In the specific NFG $\hat{N}(\mathbf{A})$, the local functions defined above explicitly forbid the value $(1, 0)$. Consequently, for every cycle formed by the underlying permutations σ_1 and σ_2 , only the realization using $(0, 1)$ edges contributes to the partition sum.

In contrast, similar to the construction of $\hat{N}(\mathbf{A})$, an NFG can be constructed such that its partition sum equals $(\text{perm}(\mathbf{A}))^2$. Crucially, the local functions of this NFG are defined such that valid configurations include simple cycles whose associated variables take the value $(0, 1)$, as well as those taking the value $(1, 0)$ that are explicitly forbidden in $\hat{N}(\mathbf{A})$. Consequently, in this unconstrained case, a cycle of length $h \geq 2$ can be realized by the edge variables in two ways: either via edges taking the value $(1, 0)$ or via edges taking the value $(0, 1)$. Both realizations contribute equally to the partition sum.

Comparing the two cases, we see that for every cycle of length $h \geq 2$, the partition sum of $\hat{N}(\mathbf{A})$ captures only one of the two possible realizations available in the NFG for the squared permanent. This effectively introduces a penalty factor of $1/2$ per cycle. Summing over all permutation pairs yields the identity [14] as

$$\frac{\text{perm}_{B,2}(\mathbf{A})}{\text{perm}(\mathbf{A})} = \sqrt{\sum_{\sigma_1, \sigma_2 \in \mathcal{S}_n} p(\sigma_1) p(\sigma_2) 2^{-c(\sigma_1 \circ \sigma_2^{-1})}}, \quad (32)$$

where $p(\sigma) \triangleq (\prod_i a_{i,\sigma(i)}) / \text{perm}(\mathbf{A})$ and $c(\sigma_1 \circ \sigma_2^{-1})$ counts the number of cycles of length > 1 in the cycle decomposition of $(\sigma_1 \circ \sigma_2^{-1})$. For full technical details, see [14].

APPENDIX B

FACTOR-GRAF VIEW OF THE TRACE KERNELS \mathbf{W} AND \mathbf{S}

This section provides a short NFG-based view behind Definitions 2–3. The goal is to justify (i) why the indeterminates \mathbf{t}, \mathbf{u} act as counting indeterminates in the generating functions, and (ii) why the relevant cycle weights collapse to trace moments $\text{tr}(\mathbf{W}^k)$ (equivalently $\text{tr}(\mathbf{S}^k)$).

A. Counting indeterminates, partitioning selection, and the weighted transition

Under Assumption 1, the $n \times n$ matrix $\mathbf{A} = \mathbf{A}(\mathbf{B}, \mathbf{k}, \mathbf{\ell})$ is expanded from the matrix $\mathbf{B} = (b_{i,j}) \in \mathbb{R}_{>0}^{m \times m}$ with fixed multiplicities $\mathbf{k}, \mathbf{\ell} \in \mathbb{Z}_{>0}^m$. To select a prescribed partitioning in a symmetry-reduced enumeration, we attach indeterminates $\mathbf{t} = (t_1, \dots, t_m)$ to row types and $\mathbf{u} = (u_1, \dots, u_m)$ to column types. Each use of a row (column) of type i (j) contributes

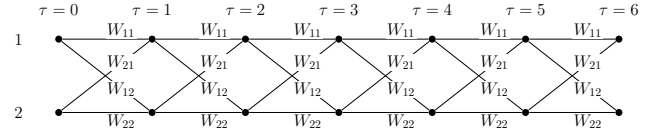


Fig. 4: Trellis graph with two states over 7 time steps.

a multiplicative factor t_i (u_j) to the total weight of the walk. Since the weight of a walk is the product of its step weights, visiting type i exactly k_i times results in the accumulation of the factor t_i to the power of k_i . Consequently, configurations associated with the partitioning $(\mathbf{k}, \mathbf{\ell})$ naturally contribute the monomial $\mathbf{t}^k \mathbf{u}^\ell$, allowing the partitioning constraints to be enforced via the coefficient extraction $[\mathbf{t}^k \mathbf{u}^\ell]$.

For the cycle-index enumeration, we need the aggregated weight of length- h closed walks on the type graph. The basic local pattern is two consecutive columns coupled through the same row. A step from a column type j to a column type j' passes through an intermediate row type i and contributes the product of the two elemental entries on that row, $b_{i,j} b_{i,j'}$, together with the counting markers t_i and $u_{j'}$. Thus the step weight is $b_{i,j} t_i b_{i,j'} u_{j'}$. Summing (marginalizing) over the intermediate row type yields the one-step kernel

$$W_{jj'} \triangleq \sum_{i \in [m]} b_{i,j} t_i b_{i,j'} u_{j'},$$

which is exactly the weighted transition matrix

$$\mathbf{W} = \mathbf{B}^\top \text{diag}(\mathbf{t}) \mathbf{B} \text{ diag}(\mathbf{u}). \quad (17)$$

Summing over all closed type sequences (j_1, \dots, j_h) with $j_{h+1} \equiv j_1$ gives the standard trace identity

$$\sum_{j_1, \dots, j_h} W_{j_1 j_2} \cdots W_{j_h j_1} = \text{tr}(\mathbf{W}^h),$$

so $\text{tr}(\mathbf{W}^h)$ packages the total weight of all length- h cycles, while \mathbf{t}, \mathbf{u} merely record the type counts.

For $m = 2$, this viewpoint can be visualized as a trellis over the column-type state space. The structure of this trellis is illustrated in Fig. 4. It consists of two states at each of the $T+1 = 7$ time steps ($\tau = 0$ to 6), with all transitions between consecutive time steps allowed. Each edge from state j to j' carries weight $W_{jj'}$. Consequently, summing the weights of all closed length- T paths in the trellis is exactly $\text{tr}(\mathbf{W}^T)$.

B. Symmetrization and the NFG kernel factorization

The weighted transition matrix \mathbf{W} in (17) is a convenient walk kernel, but it is generally not symmetric because the column-type marker $u_{j'}$ is attached to the arrival type. For the spectral manipulations used in the main text, it is preferable to pass to a real symmetric kernel without changing any trace moment $\text{tr}(\mathbf{W}^h)$.

This is done by splitting each column-type marker across the two half-edges incident to a step, i.e., replacing $u_{j'}$ by

$\sqrt{u_j}\sqrt{u_{j'}}$ at the level of a transition $j \rightarrow j'$. Equivalently, we apply the diagonal similarity transform

$$\begin{aligned} \mathbf{S}(\mathbf{t}, \mathbf{u}) &\triangleq \text{diag}(\mathbf{u})^{1/2} \mathbf{W} \text{diag}(\mathbf{u})^{-1/2} \\ &= \text{diag}(\mathbf{u})^{1/2} \mathbf{B}^\top \text{diag}(\mathbf{t}) \mathbf{B} \text{diag}(\mathbf{u})^{1/2}. \end{aligned} \quad (17)$$

Since \mathbf{S} and \mathbf{W} are similar, they preserve all trace moments,

$$\text{tr}(\mathbf{S}^h) = \text{tr}(\mathbf{W}^h), \quad h \geq 1. \quad (33)$$

Moreover, writing \mathbf{a}_j for the j -th column of \mathbf{B} , (17) yields the Gram form

$$S_{j,j'} = \sqrt{u_j u_{j'}} \langle \mathbf{a}_j, \mathbf{a}_{j'} \rangle_{\mathbf{t}}, \quad \langle \mathbf{x}, \mathbf{y} \rangle_{\mathbf{t}} \triangleq \mathbf{x}^\top \text{diag}(\mathbf{t}) \mathbf{y},$$

so whenever $\mathbf{t}, \mathbf{u} \in \mathbb{R}_{>0}^m$ (as holds in Proposition 6), the matrix $\mathbf{S}(\mathbf{t}, \mathbf{u})$ is real symmetric and positive semidefinite.

Figure 5 illustrates this procedure in NFG language. One first applies Open The Box (OTB) to the nodes representing the column indeterminates (red regions). By factorizing the column-type weight u_j symmetrically into $\sqrt{u_j}$ on the adjacent half-edges, we prepare the edges to carry the combined interaction weights. The factor node f represents the local row-mediated interaction: for a fixed intermediate row type i , it contributes the elemental weight $b_{i,j} t_i b_{i,j'}$ that couples two consecutive column types $j \rightarrow j'$ through that row type. One then applies Close The Box (CTB) to regroup the components (blue regions). Upon this regrouping, each resulting box abstracts exactly to one entry of the symmetric kernel \mathbf{S} in (17). Consequently, a length- h cycle becomes a closed sequence of h such kernel boxes, whose total contribution is $\text{tr}(\mathbf{S}^h)$ as in (33).

APPENDIX C PROOF OF PROPOSITION 6

This section provides the derivation of the asymptotic partition sums using analytic combinatorics in several variables (ACSV) [18].

First, recall the relevant setup and definitions. The generating functions for the partition sums, derived in Lemma 4, take the explicit forms as

$$C^G(\mathbf{z}) = \frac{1}{\det(\mathbf{I} - \mathbf{S}(\mathbf{z}))}, \quad (20)$$

$$C^B(\mathbf{z}) = \frac{\exp\left(\frac{1}{2} \text{tr}(\mathbf{S}(\mathbf{z}))\right)}{\sqrt{\det(\mathbf{I} - \mathbf{S}(\mathbf{z}))}}. \quad (21)$$

Here, $\mathbf{z} \triangleq (\mathbf{t}, \mathbf{u})$ denotes the collection of $2m$ indeterminates.

As established in Lemma 5, our primary quantities of interest correspond to the coefficients of these functions associated with the partitioning $\mathbf{r} \triangleq (\mathbf{k}, \ell)$ given by

$$Z_n^G(\mathbf{k}, \ell) = [\mathbf{z}^\mathbf{r}] C^G(\mathbf{z}), \quad (34)$$

$$Z_n^B(\mathbf{k}, \ell) = [\mathbf{z}^\mathbf{r}] C^B(\mathbf{z}). \quad (35)$$

To treat both cases within a unified framework, we adopt the standard ACSV form $F(\mathbf{z}) = P(\mathbf{z})Q(\mathbf{z})^{-\alpha}$. The analysis centers on the spectral properties of the symmetric transition matrix $\mathbf{S}(\mathbf{z})$. Let $\lambda_1(\mathbf{z}) \geq \lambda_2(\mathbf{z}) \geq \dots \geq \lambda_m(\mathbf{z})$ denote its eigenvalues.

When \mathbf{z} lies in the positive real orthant, Perron–Frobenius theory implies that $\lambda_1(\mathbf{z})$ is simple and strictly dominant. Hence, in the regime where $\lambda_1(\mathbf{z})$ approaches 1 while $\lambda_i(\mathbf{z}) < 1$ for $i \geq 2$, the determinant vanishes through the principal factor. We thus identify the singular function as

$$Q(\mathbf{z}) \triangleq 1 - \lambda_1(\mathbf{z}). \quad (36)$$

We effectively isolate this singularity by decomposing the determinant as

$$\det(\mathbf{I} - \mathbf{S}(\mathbf{z})) = Q(\mathbf{z}) \prod_{i=2}^m (1 - \lambda_i(\mathbf{z})). \quad (37)$$

The remaining factors constitute the analytic part $P(\mathbf{z})$. Specifically, we identify:

- Gibbs case ($\alpha=1$): The analytic part is

$$P_G(\mathbf{z}) \triangleq \prod_{i=2}^m (1 - \lambda_i(\mathbf{z}))^{-1}. \quad (38)$$

- Bethe case ($\alpha=1/2$): Using $\text{tr}(\mathbf{S}) = \sum \lambda_i$, the analytic part becomes

$$P_B(\mathbf{z}) \triangleq e^{\lambda_1(\mathbf{z})/2} \prod_{i=2}^m \frac{e^{\lambda_i(\mathbf{z})/2}}{(1 - \lambda_i(\mathbf{z}))^{1/2}}. \quad (39)$$

With the functions P , Q , and order α defined, we now proceed to analyze the geometry of the singular variety $\mathcal{V} \triangleq \{\mathbf{z} : Q(\mathbf{z}) = 0\}$.

For $\mathbf{z} \in \mathbb{R}_{>0}^{2m}$, the matrix entries of $\mathbf{S}(\mathbf{z})$ are strictly increasing in each variable. Consequently, the gradient of the Perron–Frobenius eigenvalue is nonzero, i.e., $\nabla Q(\mathbf{z}) = -\nabla \lambda_1(\mathbf{z}) \neq 0$. By the smoothness criterion in [18, Lemma 7.6], this non-vanishing gradient ensures that \mathcal{V} is smooth at any point in $\mathcal{V} \cap \mathbb{R}_{>0}^{2m}$ where $Q(\mathbf{z})=0$.

Since the generating functions have non-negative coefficients, the multivariate Vivanti–Pringsheim theorem [18, Proposition 6.38] implies that the boundary of the domain of convergence meets the positive real orthant at a minimal point $\mathbf{w} \in \mathcal{V} \cap \mathbb{R}_{>0}^{2m}$. The asymptotics in the direction \mathbf{r} are determined by the minimal smooth critical point \mathbf{w} , which we obtain by solving the smooth critical point equations [18, Lemma 7.8]

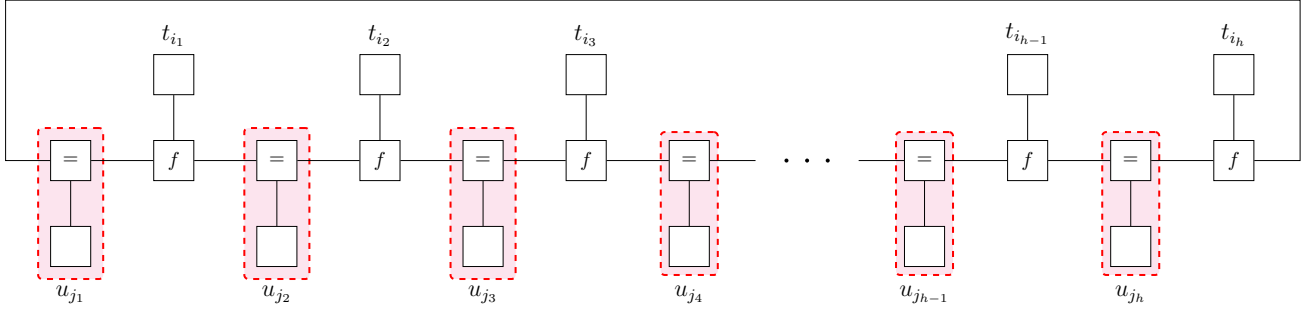
$$\begin{cases} Q(\mathbf{w}) = 0, & \text{(singularity condition)} \\ \mathbf{r} = -\eta \nabla_{\log} Q(\mathbf{w}), \quad \eta > 0. & \text{(criticality condition)} \end{cases} \quad (40)$$

Here, η is the Lagrange scaling parameter enforcing the directional constraint, and $\nabla_{\log} Q(\mathbf{w}) = (w_i \partial_{z_i} Q(\mathbf{w}))_{i=1}^{2m}$.

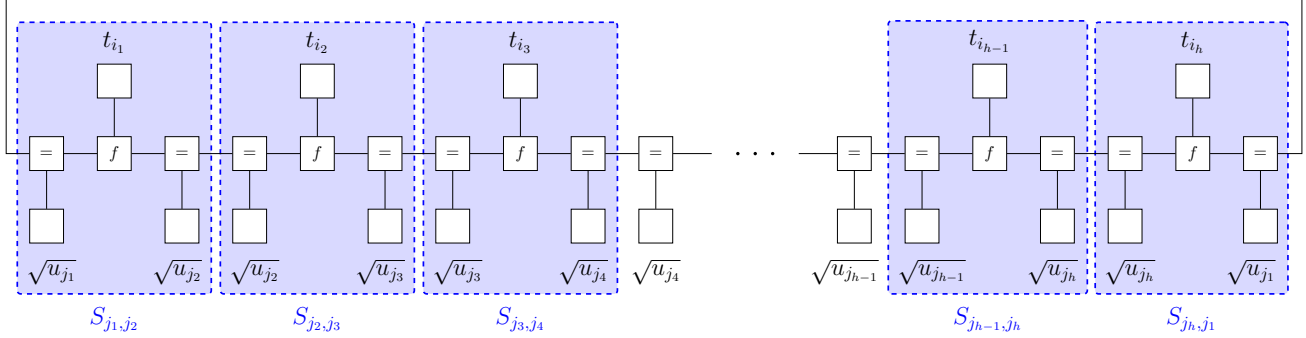
A. Proof Sketch

We briefly sketch the geometric intuition behind decomposing the multivariate integral into tangential and normal components before proceeding to the technical details.

In logarithmic coordinates $\zeta = \log \mathbf{z}$, the multivariate Cauchy integral for the coefficient $[\mathbf{z}^\mathbf{r}] F(\mathbf{z})$ localizes around the critical point \mathbf{w} . The calculation splits into two orthogonal components:



(a) NFG whose partition sum aggregates length- h closed walks on the type graph. The ν -th visited column or row contributes markers t_{i_ν} and u_{j_ν} with $i_\nu, j_\nu \in \{1, \dots, m\}$. The factor node f encodes the local elemental weight $b_{i_\nu j_\nu} t_{i_\nu} b_{i_\nu j_{\nu+1}}$ along one step. Red Open The Box (OTB) regions split each u_{j_ν} into two adjacent factors $\sqrt{u_{j_\nu}}$.



(b) After CTB (blue), each grouped box becomes a symmetric kernel entry $S_{j_\nu j_{\nu+1}}$, and the length- h cycle evaluates to $\text{tr}(\mathbf{S}^h)$ (equivalently $\text{tr}(\mathbf{W}^h)$).

Fig. 5: OTB/CTB factor-graph derivation of the kernel factorization $\mathbf{W} \mapsto \mathbf{S}$ and the trace representation of length- h closed walks.

- Tangential Integration (Gaussian): Integration over the $(d_{\text{eff}} - 1)$ directions tangent to the surface $Q = 0$ yields a Gaussian integral. This contributes the geometric pre-factor involving the determinant of the Hessian \mathcal{H} of the phase function restricted to the manifold.
- Normal Integration (Hankel): Integration over the direction normal to the surface is governed by the singularity $Q^{-\alpha}$. By introducing the local normal coordinate $q \triangleq -\tilde{Q}(\zeta)$ and deforming the path to the canonical Hankel contour \mathcal{C}_H , this component is identified with the reciprocal Gamma function via

$$-\frac{1}{2\pi i} \int_{\mathcal{C}_H} (-q)^{-\alpha} e^{-\eta q} dq = \frac{\eta^{\alpha-1}}{\Gamma(\alpha)}. \quad (41)$$

A key step in our proof is establishing that the Lagrange scaling parameter satisfies $\eta = n$. This follows directly from Euler's homogeneous function theorem, given that the Perron-Frobenius eigenvalue $\lambda_1(\mathbf{z})$ (and hence Q) is homogeneous of degree 1.

Finally, evaluating the analytic part $P(\mathbf{w})$ at the critical point and combining it with the Gaussian and Hankel factors yields the asymptotic formulas in Proposition 6.

This concludes the proof sketch. We now proceed with the detailed derivation.

B. Asymptotic Factorization via ACSV

Having established the standard form $F(\mathbf{z}) = P(\mathbf{z})Q(\mathbf{z})^{-\alpha}$ and the smoothness of the singular variety at the dominant critical point \mathbf{w} , we now evaluate the coefficient extraction integral.

Under Assumption 1, the partitioning $\mathbf{r} \triangleq (\mathbf{k}, \mathbf{\ell}) \in \mathbb{Z}_{\geq 0}^{2m}$ for admissible configurations are constrained by the global balance condition $\sum_{i=1}^m k_i = \sum_{j=1}^m \ell_j$. This implies that the support of the coefficient array lies on a codimension-one hyperplane defined by $\mathbf{c} \cdot \mathbf{r} = 0$ with $\mathbf{c} = (\mathbf{1}_m, -\mathbf{1}_m)$. Consequently, the problem possesses one redundant degree of freedom, reducing the effective dimension to

$$d_{\text{eff}} \triangleq 2m - 1. \quad (42)$$

We now formulate the integral representation for the coefficient $a_{\mathbf{r}}$ in this reduced space. To eliminate the redundancy, we parameterize the problem using d_{eff} independent variables (e.g., by eliminating $\ell_m = \sum_{i=1}^m k_i - \sum_{j=1}^{m-1} \ell_j$ and the corresponding indeterminate u_m). In the following, we let \mathbf{z} and \mathbf{r} denote these effective coordinates and partitioning, respectively. Under this convention, $a_{\mathbf{r}}$ is given by the multivariate Cauchy integral

$$a_{\mathbf{r}} = \frac{1}{(2\pi i)^{d_{\text{eff}}}} \oint_{\mathcal{C}} F(\mathbf{z}) \mathbf{z}^{-\mathbf{r}-1} dz. \quad (43)$$

Introducing logarithmic coordinates $z = \exp(\zeta)$ and setting $\tilde{P}(\zeta) \triangleq P(e^\zeta)$ and $\tilde{Q}(\zeta) \triangleq Q(e^\zeta)$, the integral transforms into the exponential form

$$a_r = \frac{1}{(2\pi i)^{d_{\text{eff}}}} \int_C \exp(-r \cdot \zeta) \tilde{P}(\zeta) \tilde{Q}(\zeta)^{-\alpha} d\zeta. \quad (44)$$

Let $\zeta^* \triangleq \log w$, where w satisfies $Q(w) = 0$. The gradients in ζ -space and in log-space agree

$$\nabla_\zeta \tilde{Q}(\zeta^*) = \nabla_{\log} Q(w).$$

Set $v \triangleq \nabla_{\log} Q(w)$ and choose an orthonormal basis $v^{(2)}, \dots, v^{(d_{\text{eff}})}$ for the tangent space at ζ^* with $v^{(j)} \perp v$. We use the local chart

$$\zeta = \zeta^* + u v + \sum_{j=2}^{d_{\text{eff}}} y_j v^{(j)}, \quad (45)$$

where u is the (unnormalized) normal coordinate and $y \triangleq (y_2, \dots, y_{d_{\text{eff}}})^\top$ are tangential coordinates. The Jacobian matrix is $J = [v, v^{(2)}, \dots, v^{(d_{\text{eff}})}]$, hence $|\det(J)| = \|v\|_2 = \|\nabla_{\log} Q(w)\|_2$, and

$$d\zeta = \|\nabla_{\log} Q(w)\|_2 du \wedge dy_2 \wedge \dots \wedge dy_{d_{\text{eff}}}.$$

Expanding \tilde{Q} around ζ^* in these coordinates gives

$$\begin{aligned} \tilde{Q}(\zeta) &= \tilde{Q}(\zeta^*) + \nabla \tilde{Q}(\zeta^*) \cdot (\zeta - \zeta^*) + O(\|\zeta - \zeta^*\|^2) \\ &= u \|v\|_2^2 + O(\|\zeta - \zeta^*\|^2) \\ &= u \|\nabla_{\log} Q(w)\|_2^2 + O(\|\zeta - \zeta^*\|^2). \end{aligned} \quad (46)$$

Therefore, to first order,

$$\begin{aligned} d\tilde{Q}(\zeta) &\approx \|\nabla_{\log} Q(w)\|_2^2 du, \\ du &\approx \frac{1}{\|\nabla_{\log} Q(w)\|_2^2} d\tilde{Q}. \end{aligned}$$

Substituting into the volume form yields the separated wedge form

$$d\zeta \approx \frac{1}{\|\nabla_{\log} Q(w)\|_2} d\tilde{Q} \wedge dy.$$

Here, we identify the tangential volume element dy (defined via the orthonormal basis) with the oriented holomorphic $(d-1)$ area form dA for $\log \mathcal{V}$, consistent with the convention in the residue formula in [18, Theorem 9.45]. This leads to the relation

$$d\zeta \approx \frac{1}{\|\nabla_{\log} Q(w)\|_2} d\tilde{Q} \wedge dA.$$

Hence, near the critical point ζ^* , the coefficient integral is approximated by

$$a_r = \frac{1}{(2\pi i)^{d_{\text{eff}}}} \int_C \frac{\exp(-r \cdot \zeta) \tilde{P}(\zeta) \tilde{Q}(\zeta)^{-\alpha}}{\|\nabla_{\log} Q(w)\|_2} d\tilde{Q}(\zeta) \wedge dA. \quad (47)$$

We now localize the Cauchy integral near the dominant critical point $\zeta^* = \log w$. Following the stratification analysis setup (e.g., [18, Theorem 9.45]), the original integration cycle is deformed (without crossing singularities) into a local tube

aligned with the geometry of the singular manifold $\mathcal{V} = \{z : Q(z) = 0\}$.

To derive the geometric and singular contributions, we expand the exponential kernel $-r \cdot \zeta$ using the local coordinate decomposition (45). Recall that $y = (y_2, \dots, y_{d_{\text{eff}}})^\top$ denotes the tangential coordinates and $q \triangleq \tilde{Q}(\zeta)$ parameterizes the normal direction. Applying the saddle-point alignment $r = -\eta \nabla_{\log} Q(w)$, we find that the phase function decouples into a linear normal component and a quadratic tangential component as

$$\begin{aligned} -r \cdot \zeta &\approx -r \cdot \zeta^* - r \cdot (\zeta - \zeta^*) \\ &\approx -r \cdot \zeta^* + \eta q - \frac{1}{2} \|r\|_2 y^\top \mathcal{H} y, \end{aligned}$$

where \mathcal{H} represents the Hessian matrix governing the curvature of the singular manifold \mathcal{V} restricted to the tangent space. This separation in the exponent implies that the integral factorizes into two orthogonal components:

Tangential Component (Geometry): Along the directions of y (where $q = 0$), the linear variation vanishes because r is a normal vector. The dominant contribution arises from the quadratic curvature term, leading to a standard Gaussian integral [18, Theorem 5.3] given by

$$\int_{\mathbb{R}^{d_{\text{eff}}-1}} \exp\left(-\frac{1}{2} \|r\|_2 y^\top \mathcal{H} y\right) dy = \sqrt{\frac{(2\pi)^{d_{\text{eff}}-1}}{\det(\|r\|_2 \mathcal{H})}}.$$

Regarding the global prefactor $(2\pi i)^{-d_{\text{eff}}}$ from the Cauchy integral, we refer to the standard saddle-point analysis in [18, Theorem 9.45]. The deformation of the integration cycle to the path of steepest descent naturally handles the imaginary units, effectively canceling the factor $i^{-(d_{\text{eff}}-1)}$ associated with the tangential dimensions. Combining the resulting real prefactor $(2\pi)^{-(d_{\text{eff}}-1)}$ with the Gaussian integral above, the net contribution from the tangential geometry is

$$\frac{1}{\sqrt{(2\pi \|r\|_2)^{d_{\text{eff}}-1} \det(\mathcal{H})}}.$$

Normal Component (Singularity): To provide a unified treatment for both algebraic singularities ($\alpha \notin \mathbb{Z}$) and polar singularities ($\alpha \in \mathbb{Z}_{>0}$), we adopt the Hankel contour framework adapted from the singularity analysis of generating functions (see, e.g., the transfer theorem in [19, Theorem VI.3]). This approach treats the singularity generically as a branch point.

To align with the standard Hankel contour definition (where the path wraps around the positive real axis), we define the normal coordinate with a sign flip as

$$q \triangleq -\tilde{Q}(\zeta) = \lambda_1(e^\zeta) - 1. \quad (48)$$

With this definition, the singular factor becomes $(-q)^{-\alpha}$. Applying the saddle-point alignment, the expansion of the exponential kernel $-r \cdot \zeta$ yields a decaying term $-\eta q$ (since $\eta > 0$).

The justification for retaining the constant prefactor $\|\nabla_{\log} Q(w)\|_2^{-1}$ in (47) relies on localizing the integral.

We first restrict the integration to a small neighborhood of ζ^* where the variations in the smooth prefactors are negligible. We then extend the path to the full Hankel contour \mathcal{C}_H , which starts and ends at $+\infty$ and winds counter-clockwise around the origin.

This extension is justified because the contribution from the added tails is exponentially small due to the decay of $e^{-\eta q}$. Furthermore, in the specific case of poles ($\alpha \in \mathbb{Z}$), the contributions from the two parallel lines of the contour along the branch cut exactly cancel, naturally recovering the standard residue result.

The normal integral thus matches the canonical representation of the reciprocal Gamma function [19, Theorem B.1] given by

$$\mathcal{I}_{\text{norm}} = -\frac{1}{2\pi i} \int_{\mathcal{C}_H} (-q)^{-\alpha} e^{-\eta q} dq.$$

By substituting $u = \eta q$, we obtain the final result

$$\mathcal{I}_{\text{norm}} = \eta^{\alpha-1} \left(-\frac{1}{2\pi i} \int_{\mathcal{C}_H} (-u)^{-\alpha} e^{-u} du \right) = \frac{\eta^{\alpha-1}}{\Gamma(\alpha)}.$$

Combining the constant amplitude $\mathbf{w}^{-r} P(\mathbf{w})$, the tangential Gaussian result, and the explicit evaluation of $\mathcal{I}_{\text{norm}}$, we obtain the final asymptotic formula

$$a_{\mathbf{r}} \sim \frac{\mathbf{w}^{-r} P(\mathbf{w})}{\sqrt{(2\pi\|\mathbf{r}\|_2)^{d_{\text{eff}}-1} \det(\mathcal{H})}} \cdot \frac{1}{\|\nabla_{\log} Q(\mathbf{w})\|_2} \cdot \frac{\eta^{\alpha-1}}{\Gamma(\alpha)}. \quad (49)$$

Remark 9. We verify the correctness of the gradient factor by checking invariance under the rescaling $Q \mapsto Q_c \triangleq cQ$ for any constant $c > 0$. Since the generating function scales as $F_c(\mathbf{z}) = P(\mathbf{z})(cQ(\mathbf{z}))^{-\alpha} = c^{-\alpha} F(\mathbf{z})$, the asymptotic coefficient must satisfy the exact scaling law

$$a_{\mathbf{r}}^{(c)} = c^{-\alpha} a_{\mathbf{r}}. \quad (50)$$

We now examine how the components of the derived asymptotic formula transform:

- The gradient norm scales linearly as $\|\nabla_{\log} Q_c(\mathbf{w})\|_2 = c \|\nabla_{\log} Q(\mathbf{w})\|_2$.
- The Lagrange multiplier η , determined by $\mathbf{r} = -\eta_c \nabla_{\log} Q_c(\mathbf{w})$, scales inversely such that $\eta_c = c^{-1} \eta$.
- Consequently, the normal Hankel integral contribution scales as

$$\frac{\eta_c^{\alpha-1}}{\Gamma(\alpha)} = c^{-(\alpha-1)} \frac{\eta^{\alpha-1}}{\Gamma(\alpha)}.$$

To recover the required total scaling $c^{-\alpha}$ in (50), the remaining geometric prefactor must contribute exactly a factor of $c^{-\alpha}/c^{-(\alpha-1)} = c^{-1}$. Since the gradient norm scales as c^1 , it must appear with power one in the denominator

$$\frac{1}{\|\nabla_{\log} Q_c(\mathbf{w})\|_2} = c^{-1} \frac{1}{\|\nabla_{\log} Q(\mathbf{w})\|_2}.$$

In contrast, a squared denominator would scale as c^{-2} , leading to an incorrect total scaling of $c^{-(\alpha+1)}$. This confirms that the formula in the first edition [20, Theorem 9.5.4] (power

one) is dimensionally consistent, whereas the expression in the second edition [18, Theorem 9.45] (squared norm) is incorrect.

It remains to identify the Lagrange multiplier η in the critical-point equations. Although the integration is carried out in effective coordinates, the algebraic characterization of the critical point is most naturally derived using the full symmetry of the transition matrix in the ambient space. From the saddle-point alignment

$$\mathbf{r} = -\eta \nabla_{\log} Q(\mathbf{w}), \quad Q(\mathbf{z}) = 1 - \lambda_1(\mathbf{z}),$$

Since $\lambda_1(\mathbf{w}) = 1$ on the manifold \mathcal{V} , the differential satisfies $d\lambda_1 = \lambda_1 d \log \lambda_1 = d \log \lambda_1$. We thus equivalently have

$$\mathbf{r} = \eta \nabla_{\log} \lambda_1(\mathbf{w}), \quad \nabla_{\log} \lambda_1(\mathbf{w}) = \frac{\partial \log \lambda_1}{\partial \log \mathbf{z}} \Big|_{\mathbf{w}}.$$

This alignment holds componentwise as

$$k_i = \eta \frac{\partial \log \lambda_1(\mathbf{t}, \mathbf{u})}{\partial \log t_i} \Big|_{(\mathbf{t}, \mathbf{u})=\mathbf{w}}, \quad i = 1, \dots, m, \quad (51)$$

$$\ell_j = \eta \frac{\partial \log \lambda_1(\mathbf{t}, \mathbf{u})}{\partial \log u_j} \Big|_{(\mathbf{t}, \mathbf{u})=\mathbf{w}}, \quad j = 1, \dots, m. \quad (52)$$

Invoking the partitioning constraints from Assumption 1, summing (51) over i and (52) over j yields

$$n = \sum_{i \in [m]} k_i = \eta \sum_{i \in [m]} \frac{\partial \log \lambda_1}{\partial \log t_i} \Big|_{\mathbf{w}}, \quad (53)$$

$$n = \sum_{j \in [m]} \ell_j = \eta \sum_{j \in [m]} \frac{\partial \log \lambda_1}{\partial \log u_j} \Big|_{\mathbf{w}}. \quad (54)$$

To evaluate the sums of logarithmic derivatives, note that the state-transition matrix $\mathbf{S}(\mathbf{t}, \mathbf{u})$ is constructed with entries proportional to the product $t_i u_j$. Consequently, \mathbf{S} is homogeneous of degree 1 in \mathbf{t} (fixing \mathbf{u}) and also of degree 1 in \mathbf{u} (fixing \mathbf{t}). Explicitly, for any $c > 0$,

$$\mathbf{S}(c\mathbf{t}, \mathbf{u}) = c \mathbf{S}(\mathbf{t}, \mathbf{u}), \quad \mathbf{S}(\mathbf{t}, c\mathbf{u}) = c \mathbf{S}(\mathbf{t}, \mathbf{u}),$$

hence the Perron–Frobenius eigenvalue scales linearly, i.e.,

$$\lambda_1(c\mathbf{t}, \mathbf{u}) = c \lambda_1(\mathbf{t}, \mathbf{u}), \quad \lambda_1(\mathbf{t}, c\mathbf{u}) = c \lambda_1(\mathbf{t}, \mathbf{u}).$$

Therefore λ_1 is a degree-1 homogeneous function in \mathbf{t} (with \mathbf{u} fixed) and likewise in \mathbf{u} (with \mathbf{t} fixed). By Euler's theorem for homogeneous functions,

$$\sum_{i \in [m]} \frac{\partial \log \lambda_1}{\partial \log t_i} \Big|_{\mathbf{w}} = 1, \quad (55)$$

$$\sum_{j \in [m]} \frac{\partial \log \lambda_1}{\partial \log u_j} \Big|_{\mathbf{w}} = 1. \quad (56)$$

Applying the Euler identity (55) and (56) to (53) and (54) uniquely determines

$$\eta = n. \quad (57)$$

This confirms that the global balance constraints align with the spectral scaling properties.

With $\eta = n$, Eq. (49) becomes

$$a_r \sim \frac{\mathbf{w}^{-r} P(\mathbf{w})}{\sqrt{(2\pi\|\mathbf{r}\|_2)^{d_{\text{eff}}-1} \det(\mathcal{H})}} \cdot \frac{1}{\|\nabla_{\log} Q(\mathbf{w})\|_2} \cdot \frac{n^{\alpha-1}}{\Gamma(\alpha)}. \quad (58)$$

Evaluating the analytic parts $P(\mathbf{w})$ at the critical point (where $\lambda_1(\mathbf{w}) = 1$, and thus $\lambda_i(\mathbf{w}) = \rho_i$ for $i \geq 2$) yields the following results:

1) *Gibbs case* ($\alpha=1$): Here $P = P_G$ with

$$P_G(\mathbf{w}) = \prod_{i=2}^m (1-\rho_i)^{-1},$$

and the normal component contribution is $\eta^0/\Gamma(1) = 1$. Thus,

$$Z_n^G \sim \frac{\mathbf{w}^{-r}}{\sqrt{(2\pi\|\mathbf{r}\|_2)^{2m-2} \det(\mathcal{H})}} \cdot \frac{\prod_{i=2}^m (1-\rho_i)^{-1}}{\|\nabla_{\log} Q(\mathbf{w})\|_2}, \quad (59)$$

which recovers the first expression in Proposition 6.

2) *Bethe double-cover case* ($\alpha=1/2$): Here $P = P_B$ and evaluating at $\lambda_1(\mathbf{w}) = 1$ gives

$$P_B(\mathbf{w}) = e^{1/2} \prod_{i=2}^m e^{\rho_i/2} (1-\rho_i)^{-1/2}.$$

The normal component contribution is

$$\frac{\eta^{-1/2}}{\Gamma(1/2)} = \frac{1}{\sqrt{\pi n}}.$$

Combining these components yields

$$Z_n^B \sim \frac{\mathbf{w}^{-r}}{\sqrt{(2\pi\|\mathbf{r}\|_2)^{2m-2} \det(\mathcal{H})}} \cdot \frac{\sqrt{\prod_{i=2}^m e^{\rho_i} (1-\rho_i)^{-1}}}{\|\nabla_{\log} Q(\mathbf{w})\|_2} \cdot \sqrt{\frac{e}{\pi n}}, \quad (60)$$

which recovers the second expression in Proposition 6.

APPENDIX D

DERIVING $(\mathbf{t}^*, \mathbf{u}^*)$ FROM SINKHORN'S THEOREM

It turns out that the ACSV saddle-point parameters $(\mathbf{t}^*, \mathbf{u}^*)$ can be obtained with the help of Sinkhorn's theorem. We restrict attention to the two-type block-constant setting $m = 2$, where $\mathbf{B} = (b_{i,j}) \in \mathbb{R}_{>0}^{2 \times 2}$ and the expanded matrix \mathbf{A} consists of four constant blocks of sizes $k_i \times \ell_j$ ($i, j \in \{1, 2\}$), with every entry in block (i, j) equal to $b_{i,j}$. Note, however, that the results in this appendix can be straightforwardly generalized to any positive integer m .

We begin by recalling the classical Sinkhorn theorem [21], which characterizes the diagonal scaling of strictly positive matrices.

Lemma 10. *For any strictly positive square matrix \mathbf{A} , there exists a unique doubly stochastic matrix \mathbf{U} expressible in the form*

$$\mathbf{U} = \mathbf{D}_1 \mathbf{A} \mathbf{D}_2, \quad (61)$$

where \mathbf{D}_1 and \mathbf{D}_2 are diagonal matrices with strictly positive diagonal entries. While \mathbf{U} is unique, the scaling matrices \mathbf{D}_1 and \mathbf{D}_2 are unique up to a common scalar factor.

Since \mathbf{U} is doubly stochastic, its row and column sums must equal 1. Combined with Eq. (61), this implies constraints on the diagonal entries of \mathbf{D}_1 and \mathbf{D}_2 . Leveraging the block-constant structure of \mathbf{A} described in Assumption 1, we can explicitly characterize these constraints.

Lemma 11. *Let \mathbf{A} be the block-constant matrix defined above. There exist positive scalars $\overrightarrow{V}_1, \overrightarrow{V}_2, \overleftarrow{V}_1, \overleftarrow{V}_2$ satisfying the coupled system*

$$\overrightarrow{V}_1 = \frac{1}{\ell_1 b_{1,1} \overleftarrow{V}_1 + \ell_2 b_{1,2} \overleftarrow{V}_2}, \quad (62)$$

$$\overrightarrow{V}_2 = \frac{1}{\ell_1 b_{2,1} \overleftarrow{V}_1 + \ell_2 b_{2,2} \overleftarrow{V}_2}, \quad (63)$$

$$\overleftarrow{V}_1 = \frac{1}{k_1 b_{1,1} \overrightarrow{V}_1 + k_2 b_{2,1} \overrightarrow{V}_2}, \quad (64)$$

$$\overleftarrow{V}_2 = \frac{1}{k_1 b_{1,2} \overrightarrow{V}_1 + k_2 b_{2,2} \overrightarrow{V}_2}, \quad (65)$$

such that the diagonal scaling matrices in (61) are given by

$$\mathbf{D}_1 = \text{diag}(\underbrace{\overrightarrow{V}_1, \dots, \overrightarrow{V}_1}_{k_1}, \underbrace{\overrightarrow{V}_2, \dots, \overrightarrow{V}_2}_{k_2}), \quad (66)$$

$$\mathbf{D}_2 = \text{diag}(\underbrace{\overleftarrow{V}_1, \dots, \overleftarrow{V}_1}_{\ell_1}, \underbrace{\overleftarrow{V}_2, \dots, \overleftarrow{V}_2}_{\ell_2}). \quad (67)$$

Proof. The block-constant structure of \mathbf{A} implies that all rows of type i are identical, as are all columns of type j . By the uniqueness of the Sinkhorn scaling, the associated diagonal factors in \mathbf{D}_1 and \mathbf{D}_2 must be uniform within each type. Substituting these uniform values into the row-sum constraint $\sum_j u_{1,j} = 1$ yields

$$\begin{aligned} 1 &= \sum_{j=1}^n \overrightarrow{V}_1 A_{1,j} (\mathbf{D}_2)_{jj} \\ &= \overrightarrow{V}_1 \left(\sum_{j \in \text{Type 1}} b_{1,1} \overleftarrow{V}_1 + \sum_{j \in \text{Type 2}} b_{1,2} \overleftarrow{V}_2 \right) \\ &= \overrightarrow{V}_1 (\ell_1 b_{1,1} \overleftarrow{V}_1 + \ell_2 b_{1,2} \overleftarrow{V}_2). \end{aligned}$$

Rearranging this equation recovers (62). The remaining equations (63)–(65) follow symmetrically from the constraints for row type 2 and both column types. \square

Theorem 12 below expresses the ACSV parameters in terms of these Sinkhorn scaling factors.

Theorem 12. *Let $m = 2$ and $\mathbf{B} \in \mathbb{R}_{>0}^{2 \times 2}$. Fix $\mathbf{r} = (k_1, k_2, \ell_1, \ell_2)$ with $k_1 + k_2 = \ell_1 + \ell_2 = n$. Let $\overrightarrow{V}_1, \overrightarrow{V}_2, \overleftarrow{V}_1, \overleftarrow{V}_2$ be the positive scalars given by Lemma 11. Construct the ACSV parameters $(\mathbf{t}^*, \mathbf{u}^*)$ explicitly as*

$$t_1^* = k_1 \overrightarrow{V}_1^2, \quad t_2^* = k_2 \overrightarrow{V}_2^2, \quad u_1^* = \ell_1 \overleftarrow{V}_1^2, \quad u_2^* = \ell_2 \overleftarrow{V}_2^2. \quad (68)$$

The choice $\mathbf{w} = (\mathbf{t}^*, \mathbf{u}^*)$ constitutes a solution to the general ACSV critical point equations (40) with scaling factor $\eta = n$. Specifically:

- **Manifold constraint:** The condition $Q(\mathbf{w}) = 0$ corresponds to the unit spectral radius requirement for the weighted transition matrix $\mathbf{W}(\mathbf{t}^*, \mathbf{u}^*)$ in Definition 2, i.e.,

$$\lambda_1(\mathbf{t}^*, \mathbf{u}^*) = 1. \quad (69)$$

- **Gradient alignment:** The condition $\mathbf{r} = -\eta \nabla_{\log} Q(\mathbf{w})$ is satisfied componentwise, meaning the scaled logarithmic derivatives of the dominant eigenvalue match the respective block dimensions. That is, with $\eta = n$, for all $i, j \in \{1, 2\}$,

$$n \frac{\partial \log \lambda_1}{\partial \log t_i} \Big|_{\mathbf{w}} = k_i, \quad n \frac{\partial \log \lambda_1}{\partial \log u_j} \Big|_{\mathbf{w}} = \ell_j. \quad (70)$$

Proof. We first define the scaling vectors

$$\vec{\mathbf{V}} \triangleq \begin{pmatrix} \vec{V}_1 \\ \vec{V}_2 \end{pmatrix}, \quad \hat{\mathbf{V}} \triangleq \begin{pmatrix} \hat{V}_1 \\ \hat{V}_2 \end{pmatrix}.$$

The Sinkhorn system (62)–(65) can be rewritten in matrix form as

$$\begin{pmatrix} \frac{1}{\vec{V}_1} \\ \frac{1}{\vec{V}_2} \end{pmatrix} = \mathbf{B} \begin{pmatrix} \ell_1 & 0 \\ 0 & \ell_2 \end{pmatrix} \hat{\mathbf{V}}, \quad (71)$$

$$\begin{pmatrix} \frac{1}{\hat{V}_1} \\ \frac{1}{\hat{V}_2} \end{pmatrix} = \mathbf{B}^T \begin{pmatrix} k_1 & 0 \\ 0 & k_2 \end{pmatrix} \vec{\mathbf{V}}. \quad (72)$$

To facilitate the analysis, we introduce the auxiliary matrix $\mathbf{M}(\mathbf{t}, \mathbf{u})$, given as

$$\begin{aligned} \mathbf{M}(t_1, t_2, u_1, u_2) &\triangleq \begin{pmatrix} \ell_1^{-1} u_1 & 0 \\ 0 & \ell_2^{-1} u_2 \end{pmatrix} \mathbf{B}^T \begin{pmatrix} k_1 & 0 \\ 0 & k_2 \end{pmatrix} \\ &\quad \cdot \begin{pmatrix} k_1^{-1} t_1 & 0 \\ 0 & k_2^{-1} t_2 \end{pmatrix} \mathbf{B} \begin{pmatrix} \ell_1 & 0 \\ 0 & \ell_2 \end{pmatrix}. \end{aligned} \quad (73)$$

Note that \mathbf{M} is similar to the weighted transition matrix $\mathbf{W}(\mathbf{t}, \mathbf{u})$ and thus shares its eigenvalues.

Next, we claim that $\phi \triangleq \vec{\mathbf{V}}$ is the right Perron eigenvector of $\mathbf{M}(\mathbf{t}^*, \mathbf{u}^*)$ with the eigenvalue 1. Substituting the constructed parameters into the definition of \mathbf{M} yields

$$\begin{aligned} \mathbf{M} \vec{\mathbf{V}} &= \begin{pmatrix} \ell_1^{-1} u_1^* & 0 \\ 0 & \ell_2^{-1} u_2^* \end{pmatrix} \mathbf{B}^T \begin{pmatrix} k_1 & 0 \\ 0 & k_2 \end{pmatrix} \\ &\quad \cdot \begin{pmatrix} k_1^{-1} t_1^* & 0 \\ 0 & k_2^{-1} t_2^* \end{pmatrix} \mathbf{B} \begin{pmatrix} \ell_1 & 0 \\ 0 & \ell_2 \end{pmatrix} \vec{\mathbf{V}} \\ &\stackrel{(a)}{=} \begin{pmatrix} \ell_1^{-1} u_1^* & 0 \\ 0 & \ell_2^{-1} u_2^* \end{pmatrix} \mathbf{B}^T \begin{pmatrix} k_1 & 0 \\ 0 & k_2 \end{pmatrix} \vec{\mathbf{V}} \\ &\stackrel{(b)}{=} \hat{\mathbf{V}}, \end{aligned}$$

where step (a) follows from applying (71) to the right-most matrix-vector product, and step (b) follows from applying (72) to the remaining expression. Thus, $\mathbf{M} \vec{\mathbf{V}} = \hat{\mathbf{V}}$, establishing that 1 is an eigenvalue of $\mathbf{M}(\mathbf{t}^*, \mathbf{u}^*)$. To identify this eigenvalue as the dominant one, we invoke the Perron–Frobenius theorem. Since \mathbf{M} is strictly positive, the Perron–Frobenius theorem implies that the spectral radius of \mathbf{M} is the unique

eigenvalue admitting a strictly positive eigenvector, and the associated positive eigenvector is unique up to scaling. Because $\vec{\mathbf{V}} > 0$ and $\mathbf{M} \vec{\mathbf{V}} = \hat{\mathbf{V}}$, we must have $\lambda_1(\mathbf{t}^*, \mathbf{u}^*) = 1$.

To analyze the gradient alignment constraints in (51)–(52), we need to compute the logarithmic derivatives of the dominant eigenvalue at $\mathbf{w} = (\mathbf{t}^*, \mathbf{u}^*)$. Define the row vector $\psi^T \triangleq (\ell_1/\vec{V}_1, \ell_2/\vec{V}_2)$. Its normalization with respect to ϕ is

$$\psi^T \phi = \left(\ell_1/\vec{V}_1 \quad \ell_2/\vec{V}_2 \right) \begin{pmatrix} \vec{V}_1 \\ \vec{V}_2 \end{pmatrix} = \ell_1 + \ell_2 = n.$$

A similar direct calculation using (71)–(72) verifies that $\psi^T \mathbf{M} = \psi^T$. Thus, ψ^T is the left Perron eigenvector of \mathbf{M} with the eigenvalue 1.

We seek to evaluate the sensitivity of the eigenvalue with respect to the parameter $\log t_1$. To this end, we define the first-order perturbation terms as

$$\tilde{\lambda}_1 \triangleq \frac{\partial \lambda_1}{\partial \log t_1}, \quad \tilde{\mathbf{M}} \triangleq \frac{\partial \mathbf{M}}{\partial \log t_1}. \quad (74)$$

Although the ACSV gradient alignment condition requires the logarithmic derivative $\partial \log \lambda_1 / \partial \log t_1$, the manifold constraint $\lambda_1(\mathbf{t}^*, \mathbf{u}^*) = 1$ ensures that this coincides with the standard derivative $\tilde{\lambda}_1$ at the solution $(\mathbf{t}^*, \mathbf{u}^*)$. We determine this value using standard eigenvalue perturbation theory (see, e.g., [22]).

Consider a small perturbation ε in the parameter $\log t_1$. This induces perturbations in the matrix $\mathbf{M} \rightarrow \mathbf{M} + \varepsilon \tilde{\mathbf{M}} + O(\varepsilon^2)$, the eigenvalue $\lambda_1 \rightarrow \lambda_1 + \varepsilon \tilde{\lambda}_1 + O(\varepsilon^2)$, and the right Perron eigenvector $\phi \rightarrow \phi + \varepsilon \tilde{\phi} + O(\varepsilon^2)$. The eigenvalue equation for the perturbed system is

$$\begin{aligned} &(\mathbf{M} + \varepsilon \tilde{\mathbf{M}} + O(\varepsilon^2))(\phi + \varepsilon \tilde{\phi} + O(\varepsilon^2)) \\ &= (\lambda_1 + \varepsilon \tilde{\lambda}_1 + O(\varepsilon^2))(\phi + \varepsilon \tilde{\phi} + O(\varepsilon^2)). \end{aligned}$$

Expanding both sides and retaining only terms linear in ε , we obtain

$$\mathbf{M}\phi + \varepsilon(\mathbf{M}\tilde{\phi} + \tilde{\mathbf{M}}\phi) \approx \lambda_1\phi + \varepsilon(\lambda_1\tilde{\phi} + \tilde{\lambda}_1\phi).$$

Since $\mathbf{M}\phi = \lambda_1\phi$, the zero-order terms cancel. Equating the coefficients of ε yields

$$\mathbf{M}\tilde{\phi} + \tilde{\mathbf{M}}\phi = \lambda_1\tilde{\phi} + \tilde{\lambda}_1\phi. \quad (75)$$

To isolate $\tilde{\lambda}_1$, we left-multiply the equation by the left Perron eigenvector ψ^T , yielding

$$\psi^T \mathbf{M} \tilde{\phi} + \psi^T \tilde{\mathbf{M}} \phi = \lambda_1 \psi^T \tilde{\phi} + \tilde{\lambda}_1 \psi^T \phi.$$

Using $\psi^T \mathbf{M} = \lambda_1 \psi^T$, the term $\lambda_1 \psi^T \tilde{\phi}$ cancels on both sides. Solving for $\tilde{\lambda}_1$, we arrive at

$$\tilde{\lambda}_1 = \frac{\psi^T \tilde{\mathbf{M}} \phi}{\psi^T \phi}. \quad (76)$$

Using the definition of $\tilde{\mathbf{M}}$ and the parameters, the numerator of the RHS of (76) becomes

$$\begin{aligned}\psi^\top \tilde{\mathbf{M}} \phi &= \psi^\top \begin{pmatrix} \ell_1^{-1} u_1^* & 0 \\ 0 & \ell_2^{-1} u_2^* \end{pmatrix} \mathbf{B}^\top \begin{pmatrix} k_1 & 0 \\ 0 & k_2 \end{pmatrix} \\ &\quad \cdot \begin{pmatrix} k_1^{-1} t_1^* & 0 \\ 0 & 0 \end{pmatrix} \mathbf{B} \begin{pmatrix} \ell_1 & 0 \\ 0 & \ell_2 \end{pmatrix} \overleftarrow{V} \\ &\stackrel{(a)}{=} k_1 \overrightarrow{V}_1 \left(\ell_1 / \overleftarrow{V}_1 \quad \ell_2 / \overleftarrow{V}_2 \right) \mathbf{B}^\top \begin{pmatrix} 1 \\ 0 \end{pmatrix} \\ &\stackrel{(b)}{=} k_1,\end{aligned}$$

where step (a) uses the relation derived in (71) that the right-most product yields $(\overrightarrow{V}_1, 0)^\top$, and step (b) simplifies the scalar product using the first component of (72). Consequently, we obtain

$$\tilde{\lambda}_1 \triangleq \frac{\psi^\top \tilde{\mathbf{M}} \phi}{\psi^\top \phi} = \frac{k_1}{n}. \quad (77)$$

This calculation yields k_1/n in the $\log t_1$ direction, confirming that the parameters derived from the Sinkhorn solution satisfy the componentwise ACSV constraint $k_1 = \eta \frac{\partial \log \lambda_1}{\partial \log t_1}$ with the scaling factor $\eta = n$. The corresponding conditions for t_2, u_1, u_2 follow immediately due to the symmetry of the setup. \square

Finally, we highlight a connection between the system of equations in Lemma 11 and the scaled Sinkhorn permanent $\text{perm}_{\text{scS}}(\mathbf{A})$. Since the parameters \overrightarrow{V}_i and \overleftarrow{V}_j are precisely the scaling factors in Sinkhorn's matrix-scaling iterations, the ACSV critical point (t^*, u^*) is intrinsically linked to the value of $\text{perm}_{\text{scS}}(\mathbf{A})$.

We start by introducing the Sinkhorn permanent and its scaled variant. Fundamentally, these quantities are rooted in a variational framework. We refer the reader to [8] and [9] for the explicit expressions of the Sinkhorn permanent $\text{perm}_{\text{S}}(\mathbf{A})$ and the scaled Sinkhorn permanent $\text{perm}_{\text{scS}}(\mathbf{A})$ as the minima of the unscaled and scaled Sinkhorn free energy minimization problems, respectively. Following the notation in [23], the scaled Sinkhorn permanent is related to the (unscaled) Sinkhorn permanent by the scaling factor e^{-n} , i.e.,

$$\text{perm}_{\text{scS}}(\mathbf{A}) \triangleq e^{-n} \cdot \text{perm}_{\text{S}}(\mathbf{A}). \quad (78)$$

Rearranging terms in (61) yields the decomposition $\mathbf{A} = \mathbf{D}_1^{-1} \mathbf{U} \mathbf{D}_2^{-1}$. Based on this factorization, the Sinkhorn approximation is defined as the product of the permanents of these inverse scaling matrices, i.e., $\text{perm}_{\text{S}}(\mathbf{A}) \triangleq \text{perm}(\mathbf{D}_1^{-1}) \cdot \text{perm}(\mathbf{D}_2^{-1})$. Since the exact permanent factorizes as $\text{perm}(\mathbf{A}) = \text{perm}_{\text{S}}(\mathbf{A}) \text{perm}(\mathbf{U})$, the accuracy of this approximation depends entirely on the permanent of the doubly stochastic matrix \mathbf{U} . Utilizing the established bounds $n!/n^n \leq \text{perm}(\mathbf{U}) \leq 1$ [24], [25], the range for the ratio of the permanent of \mathbf{A} to its scaled Sinkhorn approximation is

$$e^n \cdot \frac{n!}{n^n} \leq \frac{\text{perm}(\mathbf{A})}{\text{perm}_{\text{scS}}(\mathbf{A})} \leq e^n, \quad (79)$$

where the lower bound scales as $e^n n! / n^n \approx \sqrt{2\pi n}$ by Stirling's formula.

With these results, we can rewrite the exact asymptotic expressions for Z_n^G and Z_n^B in Proposition 6.

Proposition 13. *Let m be a positive integer. As $n \rightarrow \infty$, we can rewrite $Z_n^G(\mathbf{k}, \ell)$ and $Z_n^B(\mathbf{k}, \ell)$ in Proposition 6 as*

$$Z_n^G \sim \frac{n \cdot \mathbf{k}^{-\mathbf{k}} \ell^{-\ell} \cdot e^{2n} \cdot (\text{perm}_{\text{scS}}(\mathbf{A}))^2}{\|\mathbf{r}\|_2 (2\pi \|\mathbf{r}\|_2)^{m-1} \sqrt{\det(\mathcal{H})}} \cdot \prod_{i=2}^m \frac{1}{1-\rho_i}, \quad (80)$$

$$Z_n^B \sim \frac{n \cdot \mathbf{k}^{-\mathbf{k}} \ell^{-\ell} \cdot e^{2n} \cdot (\text{perm}_{\text{scS}}(\mathbf{A}))^2}{\|\mathbf{r}\|_2 (2\pi \|\mathbf{r}\|_2)^{m-1} \sqrt{\det(\mathcal{H})}} \cdot \sqrt{\prod_{i=2}^m \frac{e^{\rho_i}}{1-\rho_i}} \cdot \sqrt{\frac{e}{\pi n}}. \quad (81)$$

Here, $\|\mathbf{r}\|_2 = \sqrt{\sum_{i \in [m]} k_i^2 + \sum_{j \in [m]} \ell_j^2}$, $\det(\mathcal{H})$ denotes the determinant of the Hessian of the constraint function restricted to the tangent space, and $\rho_i = \lambda_i / \lambda_1$ are the spectral ratios.

Proof. We evaluate the components of the general ACSV expansion directly. First, substituting the Sinkhorn parametrizations $t_i^* = k_i \overrightarrow{V}_i^2$ and $u_j^* = \ell_j \overleftarrow{V}_j^2$ given in (68) into the saddle-point contribution $\mathbf{w}^{-\mathbf{r}}$, we obtain

$$\begin{aligned}\mathbf{w}^{-\mathbf{r}} &= \mathbf{k}^{-\mathbf{k}} \ell^{-\ell} \left(\prod_{i \in [m]} \overrightarrow{V}_i^{-k_i} \prod_{j \in [m]} \overleftarrow{V}_j^{-\ell_j} \right)^2 \\ &= \mathbf{k}^{-\mathbf{k}} \ell^{-\ell} (\text{perm}_{\text{S}}(\mathbf{A}))^2 \\ &= \mathbf{k}^{-\mathbf{k}} \ell^{-\ell} \cdot e^{2n} (\text{perm}_{\text{scS}}(\mathbf{A}))^2.\end{aligned} \quad (82)$$

Next, the gradient alignment conditions (51) and (52) imply $\nabla_{\log Q}(\mathbf{w}) = -\mathbf{r}/n$. Consequently, the gradient norm simplifies to $\|\nabla_{\log Q}(\mathbf{w})\|_2 = \|\mathbf{r}\|_2/n$.

For the spectral components, the matrix \mathbf{M} shares the same non-zero eigenvalues $\{\lambda_i\}_{i=1}^m$ with \mathbf{W} in Definition 2 and \mathbf{S} in Definition 3. At the critical point, the dominant eigenvalue is $\lambda_1 = 1$. We define the spectral ratios as $\rho_i \triangleq \lambda_i / \lambda_1$ (where $\rho_i = \lambda_i$ since $\lambda_1 = 1$) for $i = 2, \dots, m$. The resulting spectral factors are then given by $\prod_{i=2}^m (1-\rho_i)^{-1}$ for Z_n^G and $\sqrt{\prod_{i=2}^m e^{\rho_i} (1-\rho_i)^{-1}}$ for Z_n^B .

Finally, the effective dimension of the integral is $d_{\text{eff}} = 2m-1$. Combining the geometric factor $\sqrt{(2\pi \|\mathbf{r}\|_2)^{2m-2} \det(\mathcal{H})}$ with the gradient norm contribution $\|\mathbf{r}\|_2/n$ leads to the effective global prefactor

$$\frac{n}{\|\mathbf{r}\|_2 (2\pi \|\mathbf{r}\|_2)^{m-1} \sqrt{\det(\mathcal{H})}}.$$

Multiplying this prefactor by the main term and the respective spectral factors establishes the asymptotic formulas. \square

With the explicit asymptotic forms for the coefficients Z_n^G and Z_n^B established in Proposition 13, we now translate these results back to the Gibbs permanent and Bethe double-cover permanent. The following lemma combines the ACSV outcomes with the factorial relations derived in Lemma 5 to yield the final asymptotic formulas.

Lemma 14. *Let m be a positive integer. By combining the exact combinatorial relations in Lemma 5 with the asymptotic expansions in Proposition 13, it holds that*

$$\frac{(\text{perm}(\mathbf{A}))^2}{(\text{perm}_{\text{scS}}(\mathbf{A}))^2} \sim \frac{2\pi n \sqrt{\mathbf{k}^1 \ell^1}}{\|\mathbf{r}\|_2^m \sqrt{\det(\mathcal{H})}} \cdot \prod_{i=2}^m \frac{1}{1-\rho_i}, \quad (83)$$

$$\frac{(\text{perm}_{\text{B},2}(\mathbf{A}))^2}{(\text{perm}_{\text{scS}}(\mathbf{A}))^2} \sim \frac{2\pi n \sqrt{\mathbf{k}^1 \ell^1}}{\|\mathbf{r}\|_2^m \sqrt{\det(\mathcal{H})}} \cdot \sqrt{\frac{e}{\pi n}} \cdot \sqrt{\prod_{i=2}^m \frac{e^{\rho_i}}{1-\rho_i}}, \quad (84)$$

where $\|\mathbf{r}\|_2 = \sqrt{\sum_{i \in [m]} k_i^2 + \sum_{j \in [m]} \ell_j^2}$, $\rho_i = \lambda_i / \lambda_1$ denote the spectral ratios defined in Proposition 13, and we use the multi-index notation $\mathbf{x}^1 \triangleq \prod_i x_i$ (with $\mathbf{1}$ denoting the all-one vector).

Proof. Recall from Lemma 5 that

$$(\text{perm}(\mathbf{A}))^2 = \mathbf{k}! \cdot \ell! \cdot Z_n^G(\mathbf{k}, \ell).$$

Applying Stirling's approximation $n! \sim \sqrt{2\pi n}(n/e)^n$ to $\mathbf{k}!$ and $\ell!$, we obtain

$$\mathbf{k}! \cdot \ell! \sim (2\pi)^m \cdot \sqrt{\mathbf{k}^1 \ell^1} \cdot \mathbf{k}^{\mathbf{k}} \ell^{\ell} \cdot e^{-2n}, \quad (85)$$

where we used $\sum_{i \in [m]} k_i + \sum_{j \in [m]} \ell_j = 2n$.

Substituting the explicit asymptotic formula for Z_n^G from (80) into this product, we observe that the terms $\mathbf{k}^{\mathbf{k}} \ell^{\ell} e^{-2n}$ perfectly cancel the terms $\mathbf{k}^{-\mathbf{k}} \ell^{-\ell} e^{2n}$ arising from the ACSV expansion. Collecting the remaining geometric terms and simplifying $(2\pi)^m / (2\pi)^{m-1}$ to 2π yields the expression in (83). The derivation for $(\text{perm}_{\text{B},2}(\mathbf{A}))^2$ follows an identical procedure using (81). \square

To conclude, we highlight two methodological contributions of this derivation beyond the standard ACSV framework. First, our analysis explicitly identifies the effective dimension of the problem. The global constraints inherent in the block-model formulation impose a dependency among the variables, reducing the effective degrees of freedom for the coefficient extraction integral. Correctly incorporating this reduction into the geometric prefactor is crucial for obtaining the exact asymptotic magnitude. Second, the explicit comparison between Z_n^G and Z_n^B involves a non-integer exponent shift. While such cases generally fall under the scope of algebraic generating functions in ACSV theory, our derivation adopts a distinct approach by explicitly isolating the singular direction. This separation allows us to resolve the scaling behaviors using classical singularity analysis results in [19]. Specifically, this approach captures the additional decay factor of $n^{-1/2}$ in Z_n^B relative to Z_n^G , revealing the precise asymptotic difference between the two components.